


 Cite this: *RSC Adv.*, 2022, **12**, 12672

Recent advances in the application of magnetic bio-polymers as catalysts in multicomponent reactions

Zohreh Kheilkordi, ^a Ghodsi Mohammadi Ziarani, ^{*a} Fatemeh mohajer, ^a Alireaza Badiei ^b and Mika Sillanpää^{cde}

Magnetic nanoparticles have attracted significant attention due to their high surface area and superparamagnetic properties. Bio-polymers composed of polysaccharides including alginate, cellulose, glucose, dextrin, chitosan, and starch can be immobilized on magnetic nanoparticles. Bio-polymers can be obtained from natural sources, such as plants, tunicates, algae, and bacteria. Bio-polymers obtained from natural sources have attracted attention due to their various properties including efficient functional groups, non-toxicity, low cost, availability, and biocompatibility. According to the targets of "green chemistry", the application of bio-polymers is effective in reducing pollution. Furthermore, they are excellent agents for the functionalization of magnetic nanoparticles to yield nanomagnetic bio-polymers, which can be applied as recoverable and eco-friendly catalysts in multicomponent reactions.

Received 25th February 2022

Accepted 7th April 2022

DOI: 10.1039/d2ra01294d

rsc.li/rsc-advances

1. Introduction

Among the various magnetic nanoparticles, nano magnetic iron oxide (Fe_3O_4) is very important because of its low cost, easy synthesis, and high magnetic ability. Recently, magnetic nanoparticles have been extensively applied in various fields including drug delivery, sensing, water treatment, removal of heavy metals, and catalysis. However, they are unstable in alkaline and acidic media due to the easy oxidation of their surface area.^{1–8} These drawbacks can be alleviated *via* the modification of Fe_3O_4 nanoparticles with materials such as silanes,^{9,10} activated carbon,¹¹ and biocompatible polymers.^{12,13} Another class of magnetic nanoparticles is ferrite magnetic nanomaterials and hexaferrite (M-type). Ferrite magnetic nanomaterials and hexaferrite have various applications including high chemical strength materials, home appliances, supercapacitors, loudspeakers, electromagnetic wave absorption, and permanent magnets.^{14–18} Overall, due to the properties of ferrite magnetic nanomaterials and hexaferrite (M-type), they

can be used for the adsorption of various metals ions, cationic and anionic dyes from wastewater.^{19–23}

The design and synthesis of biocompatible magnetic nanoparticles are important subjects in green chemistry.²⁴ Bio-polymers including alginate, cellulose, glucose, dextrin, chitosan, and starch are known as polysaccharides, which are present in the carbohydrates in plants, animals, microbes, and algae (Fig. 1).²⁴ These bio-polymers have different properties such as biodegradable nature, biocompatibility, non-toxicity, availability, low cost, and heat resistance.²⁵ They are excellent agents for the functionalization of magnetic nanoparticles to yield nanomagnetic bio-polymers, promoting their longevity, hardness, and strength. These composites have many applications such as drug delivery,^{26–28} chemotherapy,^{29,30} magnetic resonance imaging (MRI) agents,^{31,32} solar cells,³³ chemical sensors,^{34,35} catalysts,³⁶ water treatment,^{37,38} and biomedical sensors.³⁹

In comparison to conventional catalysts, heterogeneous magnetic bio-polymers have various advantages such as non-toxicity, easy separation, and eco-friendly nature. According to the functional groups on the magnetic nanoparticles, the catalysts can be grouped in various categories including, Lewis and Brønsted acids and bases.^{40,41} In continuation of our research,^{42–44} in this review, the importance of nanomagnetic bio-polymers is studied in multicomponent reactions. Multicomponent reactions (MCRs) are essential tools in medicinal and organic chemistry, which have various advantages including simplicity, easy workup, availability, and reduced generation of waste. Hence, the design and application of MCRs for the synthesis of organic compounds are highly important.^{45–50}

^aDepartment of Chemistry, Faculty of Physics and Chemistry, Alzahra University, Tehran, Iran, 1993893979. E-mail: gmohammadi@alzahra.ac.ir; Fax: +98 2188613937; Tel: +98 2188613937

^bSchool of Chemistry, College of Science, University of Tehran, Tehran, Iran

^cDepartment of Chemical Engineering, School of Mining, Metallurgy and Chemical Engineering, University of Johannesburg, P. O. Box 17011, Doornfontein 2028, South Africa. E-mail: Mika.Sillanpaa@uef.fi

^dDepartment of Applied Physics, Faculty of Science and Technology, Universiti Kebangsaan Malaysia, 43600 Bangi, Selangor, Malaysia

^eInternational Research Centre of Nanotechnology for Himalayan Sustainability (IRCNHS), Shoolini University, Solan, 173212, Himachal Pradesh, India



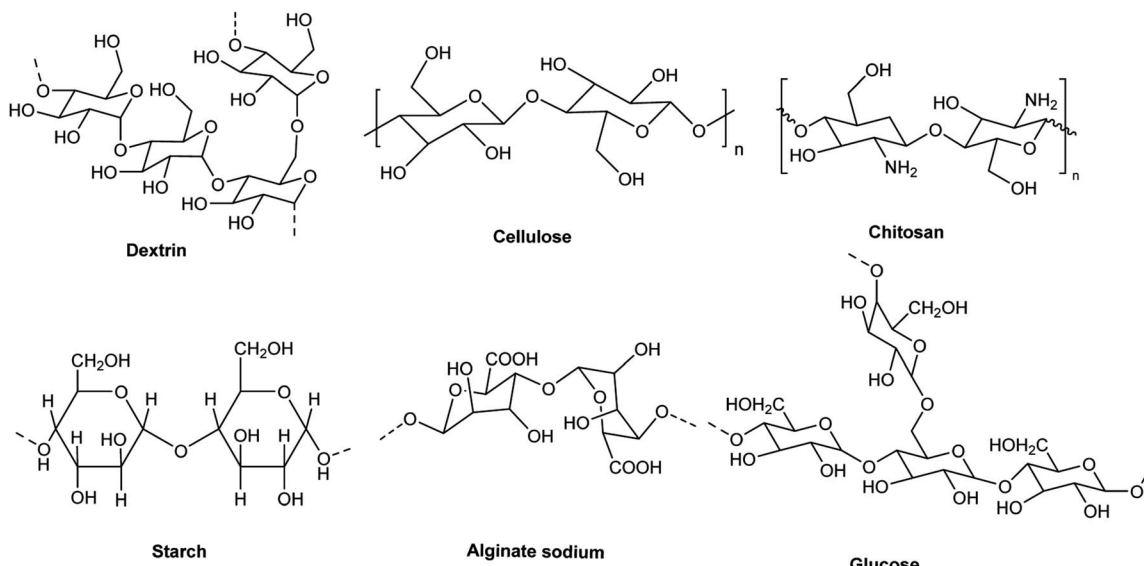


Fig. 1 Various bio-polymers.

2. Synthesis of various magnetic bio polymers

2.1. Magnetic bio-polymers based on cellulose

2.1.1. Synthesis and application of $\text{Fe}_3\text{O}_4/\text{cellulose/Co-MOF}$ nanocomposite. Initially, Fe_3O_4 nanoparticles 4 were modified with cellulose 5 using urea 6/ NaOH 7 to provide $\text{Fe}_3\text{O}_4/\text{cellulose}$ 8, which was reacted with $\text{Co}(\text{NO}_3)_2 \cdot 6\text{H}_2\text{O}$ 9, terephthalic acid 10, and imidazole (IM) 11 in DMF to form $\text{Fe}_3\text{O}_4/\text{cellulose/Co-MOF}$ nanocomposite 12 (Scheme 1).⁵¹

$\text{Fe}_3\text{O}_4/\text{cellulose/Co-MOF}$ 12 has two sites including Lewis acidic sites (Co^{2+}) and basic sites (IM), which were used in the Knoevenagel condensation reaction of aromatic aldehydes 13 with malononitrile 14 under solvent-free conditions (Scheme 2). This catalyst was reused five times without a decrease its catalytic activity.⁵¹

2.1.2. Synthesis and application of $\text{Fe}_3\text{O}_4@\text{NCS/Sb(v)}$. Initially, raw cotton was converted to nano-cellulose (NCS) 5 in the presence of NaOH 7, NaClO 16, and H_2SO_4 17 at 80°C . Then, Fe_3O_4 was functionalized with nano-cellulose (NCS) 5, providing $\text{Fe}_3\text{O}_4@\text{NCS}$ 8. In the next step, SbCl_5 was mixed with the reaction mixture in chloroform to provide $\text{Fe}_3\text{O}_4@\text{NCS/Sb(v)}$ 18 (Scheme 3).⁵²

$\text{Fe}_3\text{O}_4@\text{NCS/Sb(v)}$ was used as a Lewis acid for the activation of carbonyl groups, which was investigated in the synthesis of 4*H*-pyrimido[2,1-*b*]benzothiazoles 22 *via* the three-component reaction of aldehydes 19, 2-aminobenzothiazole 20, and ethyl acetoacetate 21 under solvent-free conditions at 90°C (Scheme 4). This catalyst was used five times without loss in its catalytic activity, which was compared with Fe_3O_4 with 39% yield in 3 h.⁵²

2.1.3. Synthesis and application of $\text{Fe}_3\text{O}_4@\text{NFC}@\text{Co(II)}$. Fe_3O_4 MNPs were synthesized *via* the reaction of $\text{FeCl}_3 \cdot 6\text{H}_2\text{O}$ and $\text{FeSO}_4 \cdot 7\text{H}_2\text{O}$ in the presence of NH_4OH solution at 80°C under an N_2 atmosphere. The Fe_3O_4 nanoparticles were dispersed in H_2O , and then nanofiber cellulose (NFC) 24 was

added to the reaction mixture at room temperature to obtain $\text{Fe}_3\text{O}_4@\text{NFC}$ 25 precipitate, which was reacted with an ethanolic solution of cobalt(II) acetate to form $\text{Fe}_3\text{O}_4@\text{NFC}@\text{Co(II)}$ 26 (Scheme 5).⁵³

Its catalytic activity was useful for the synthesis of 4*H*-pyrans *via* the multicomponent reaction of aldehydes, ethyl acetoacetate, and malononitrile in H_2O (Scheme 6).⁵³

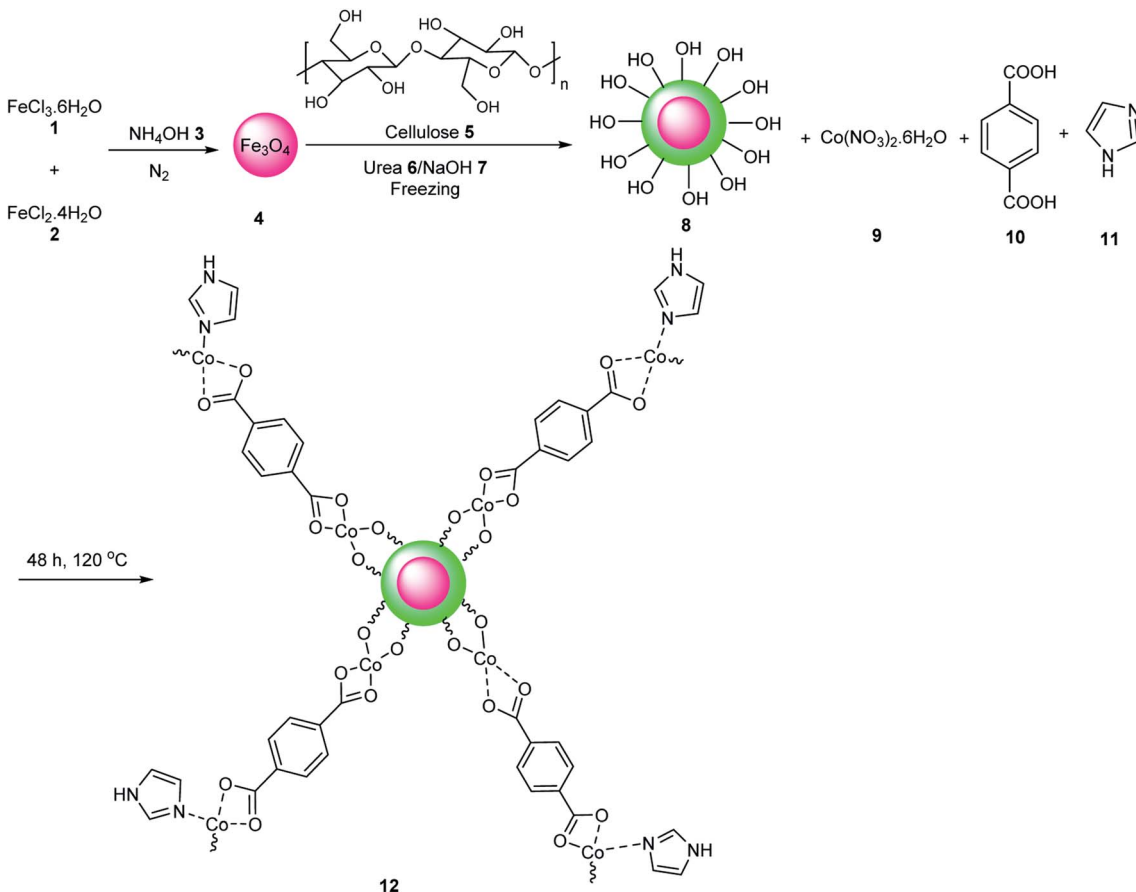
Also, the catalytic activity of 26 was tested for the synthesis of pyranopyrazole derivatives 29 *via* the four-component reaction of hydrazine hydrate 28, ethyl acetoacetate 21, benzaldehyde 19, and malononitrile 14 in H_2O (Scheme 7). The metal ions on the catalyst surface act as Lewis acids, which were activated by the malononitrile and carbonyl groups. Also, the catalyst was used five times in the model reaction without a reduction in activity.⁵³

2.1.4. Synthesis and application of cellulose@pumice. Initially, the microcrystalline cellulose was mixed with a solution of NaOH 7 and urea 6 in H_2O , and then was cooled in an ice bath at 8°C to form a gel solution, which was mixed with pumice powder 32 and stirred for 24 h to obtain cellulose@pumice 33 (Scheme 8).⁵⁴

Cellulose@pumice as an acidic catalyst activated carbonyl groups in the synthesis of 2,4,5-triarylimidazoles 36 through the reaction of benzaldehyde 19 and ammonium acetate 35 in EtOH under ultrasonic irradiation (Scheme 9). In the reusability test, this catalyst was used ten times without a reduction in activity.⁵⁴

2.1.5. The synthesis and application of $(\text{Fe}_3\text{O}_4@\text{NFC}@\text{NSalophCu})\text{CO}_2\text{H}$. Nanofiber cellulose 37 was functionalized with Fe_3O_4 *via* the sol-gel method to give $\text{Fe}_3\text{O}_4@\text{NFC}$ nanoparticles 39, which were functionalized with (3-amino-propyl)triethoxysilane (APTES) 40 to obtain $\text{Fe}_3\text{O}_4@\text{NFC}@@\text{APTES}$ 41. The reaction of salicylaldehyde 42, paraformaldehyde 43, and HCl solution under reflux conditions provided 5-chloromethyl salicylaldehyde 44, which was reacted with 3,5-diaminobenzoic acid 45 in CH_2Cl_2 at room temperature to give the Schiff base 3,5-bis((*E*)-5-(chloromethyl)-2-





Scheme 1 Synthesis of Fe_3O_4 /cellulose/Co-MOF nanocomposite 12.

hydroxybenzylidene)amino) benzoic acid ($(5\text{-Cl-Saloph})\text{CO}_2\text{H}$) **46**, followed by reaction with copper acetate in EtOH at room temperature to obtain complex $[(5\text{-Cl-Saloph})\text{Cu}(\text{II})]\text{CO}_2\text{H}$ **47**. Finally, the reaction of $[(5\text{-Cl-Saloph})\text{Cu}(\text{II})]\text{CO}_2\text{H}$ complex **47** and Fe_3O_4 @NFC@APTES **41** at $70\text{ }^\circ\text{C}$ for 24 h gave $(\text{Fe}_3\text{O}_4$ @NFC@NSalophCu) CO_2H **48** (Scheme 10).⁵⁵

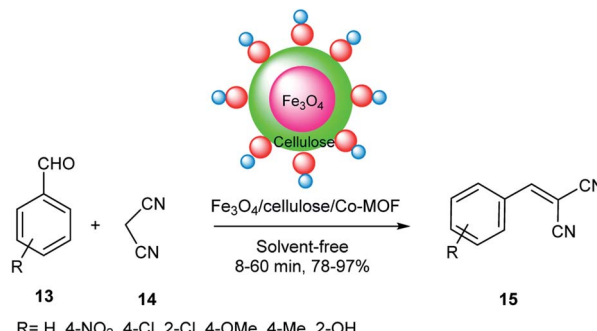
$(\text{Fe}_3\text{O}_4$ @NFC@NSalophCu) CO_2H **48** was tested in the synthesis of 5-substituted-1*H*-tetrazole **51** *via* the multicomponent reaction of various aldehydes **19**, hydroxylamine **49**, and sodium azide **50** (Scheme 11), and also in the synthesis of 1-substituted-1*H*-tetrazoles **54** *via* the multicomponent reaction of aniline **52**, triethyl orthoformate **53**, and sodium azide **50** (Scheme 12). This catalyst was used in the click reaction four times without a decrease in its activity. In this catalyst, copper metal plays a vital role in the click reactions.⁵⁵

2.1.6. Synthesis and application of Fe_3O_4 @NFC@NNSM-Mn(III). Fe_3O_4 nanoparticles were functionalized with NFC nanospheres to prepare Fe_3O_4 @NFC **39**, which was dispersed in toluene, and then 3-chloropropyl-trimethoxy silane **55** was added to the reaction mixture under N_2 gas and reflux conditions to obtain Fe_3O_4 @NFC-Cl **56**, followed by reaction with *o*-phenylenediamine **54** in CH_2Cl_2 under reflux conditions to give Fe_3O_4 @NFC@NN **57**. Then, 5-(chloromethyl)-2-hydroxy benzaldehyde **58** was reacted with Fe_3O_4 @NFC@NN **57** to form Fe_3O_4 @NFC@NNS **59**, which was complexed with

$\text{Mn}(\text{OAc})_3 \cdot 2\text{H}_2\text{O}$ **60** in EtOH to prepare Fe_3O_4 @NFC@NNS-Mn **61**, followed by reaction with melamine **62** in the presence of triethylamine in MeOH to generate Fe_3O_4 @NFC@NNSM-Mn(III) **63** (Scheme 13).⁵⁶

The activity of Fe_3O_4 @NFC@NNSM-Mn(III) **63** was tested for the synthesis of xanthenes **65** *via* the pseudo-three-component reaction of aldehydes **19** and dimedone **64** in EtOH at $45\text{ }^\circ\text{C}$ (Scheme 14). The manganese metal on the surface of Fe_3O_4 @NFC@NNSM-Mn(III) acts as a Lewis acid to activate the carbonyl groups. This catalyst was used five times without a decrease in its activity.⁵⁶

2.1.7. Synthesis and application of Fe_3O_4 @NFC@ONS-Ni(II). Initially, Fe_3O_4 @NFC **39** was functionalized with 3-chloropropyl-trimethoxy silane **55** to obtain Fe_3O_4 @NFC@CPTMS **56**. Subsequently, 2-hydroxy 4-chloromethyl benzaldehyde **44** was prepared *via* the reaction of salicylaldehyde **42**, paraformaldehyde **43**, and HCl 37% in the presence of H_2SO_4 as a catalyst at $70\text{ }^\circ\text{C}$ for 20 h. In the next step, the Schiff base ligand was synthesized *via* the reaction of 2-aminophenol **66** and 5-chloromethylsalicylaldehyde **67** in dichloromethane at $40\text{ }^\circ\text{C}$ for 3 h. Then, Fe_3O_4 @NFC@ONS **68** was obtained through the reaction of 4-(chloromethyl)-2-((2-hydroxyphenyl)imino)methyl phenol **67** and Fe_3O_4 @NFC@CPTMS **68** in the presence of triethylamine in acetonitrile under reflux conditions. In the next step, Fe_3O_4 @NFC@ONS **68** was reacted with $\text{Ni}(\text{OAc})_2$



Scheme 2 Knoevenagel condensation in the presence of Fe_3O_4 /cellulose/Co-MOF 12.

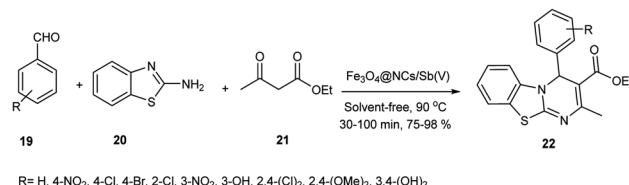
in EtOH at room temperature for 12 h to obtain $\text{Fe}_3\text{O}_4@$ NFC@ONS-Ni(II) 69. Finally, $\text{Fe}_3\text{O}_4@$ NFC@ONS-Ni(II) 70 was synthesized as a nanocatalyst *via* the reaction of $\text{Fe}_3\text{O}_4@$ NFC@ONS-Ni(II) 69 and melamine 62 in the presence of triethylamine in the MeOH under reflux conditions and N_2 gas for 12 h (Scheme 15).⁵⁷

This catalyst was used in the synthesis of polyhydroquinolines 72 through the Hantzsch reaction among benzaldehydes 19, dimedone 64, ethyl acetoacetate 21, and ammonium acetate 71 (Scheme 16).⁵⁷

Also, Bagherzade *et al.* applied this catalyst in the synthesis of 1,4-dihydropyridine 72 *via* the multicomponent reaction of aldehydes 19, ethyl acetoacetate 21, and ammonium acetate 71 (Scheme 17). The carbonyl groups in the multi-component reaction were activated in the presence of nickel metal on the surface of $\text{Fe}_3\text{O}_4@$ NFC@ONS-Ni(II) as a Lewis acid. Also, this catalyst was tested 6 times without loss in its activity.⁵⁷

2.1.8. Synthesis and application of cell-LA-TEA⁺/ Fe_3O_4 .

Initially, cellulose 5 was reacted with tosyl chloride 74 in the



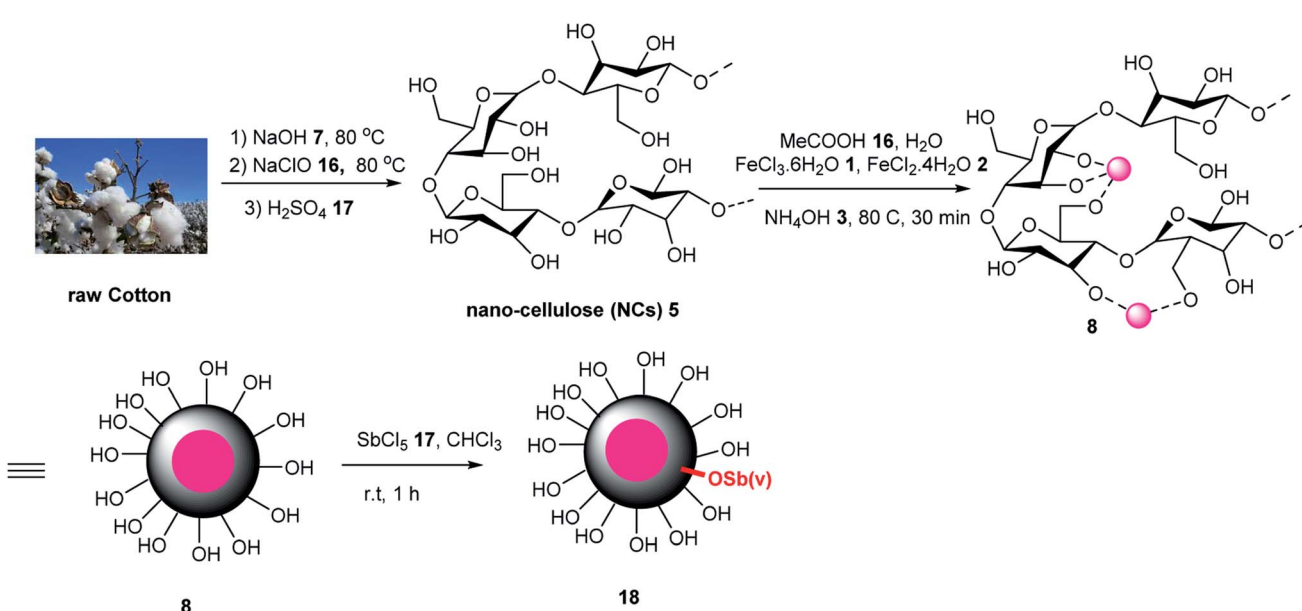
Scheme 4 Synthesis of 4H-pyrimido[2,1-b]benzothiazole derivatives 22.

presence of Et_3N to form cell-tosyl 75, which was reacted with lactic acid 76 to produce cell-LA 77, followed by reaction with triethanolamine 78 to prepare cell-LA-TEA⁺ 79. Finally, cell-LA-TEA⁺ 79 was magnetized *via* the reaction of $\text{FeCl}_3 \cdot 6\text{H}_2\text{O}$, $\text{FeCl}_2 \cdot 4\text{H}_2\text{O}$, and ammonium solution in aqueous media to form cell-LA-TEA⁺/ Fe_3O_4 80 (Scheme 18).⁵⁸

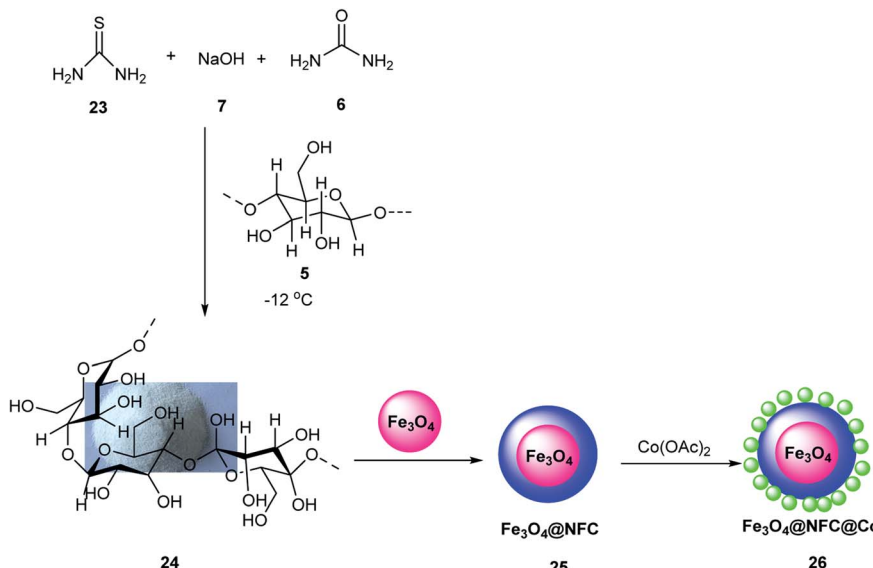
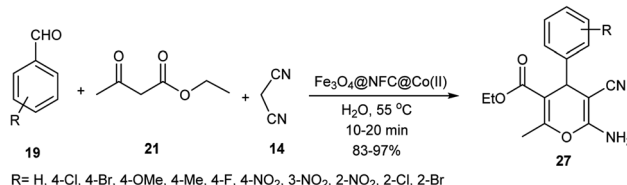
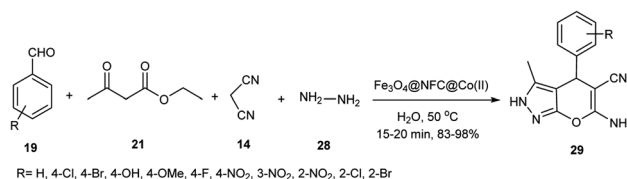
Cell-LA-TEA⁺/ Fe_3O_4 was used as a catalyst for the regioselective synthesis of pyrazolo quinolones 82 *via* the three-component reaction of dimedone 64, 5-amino pyrazolone 81, and aromatic aldehydes 19 in EtOH/H₂O under ultrasonic irradiation (Scheme 19). The catalyst was used with high stability in 7 cycles without loss in its activity.⁵⁸

2.1.9. Synthesis and application of $\text{Fe}_3\text{O}_4@$ nano-cellulose-OPO₃H. Initially, nano-cellulose 5 was prepared from cotton. Then, $\text{Fe}_3\text{O}_4@$ nano-cellulose ($\text{Fe}_3\text{O}_4@$ NCS) 8 was obtained through the reaction of nano-cellulose solution in acetic acid with $\text{FeCl}_3 \cdot 6\text{H}_2\text{O}$, $\text{FeCl}_2 \cdot 4\text{H}_2\text{O}$, and ammonium hydroxide at 80 °C. Finally, $\text{Fe}_3\text{O}_4@$ NCS were immobilized with P_4O_{10} at room temperature under grinding conditions to produce $\text{Fe}_3\text{O}_4@$ NCS-PA 83 (Scheme 20).⁵⁹

2,3-Dihydroquinazolin-4(1H)-ones 85 were prepared *via* the condensation reaction of 2-aminobenzamide 84 and aldehydes 19 in the presence of $\text{Fe}_3\text{O}_4@$ NCS-PA 83 as a Brønsted acid in H₂O: EtOH under reflux conditions (Scheme 21). The main

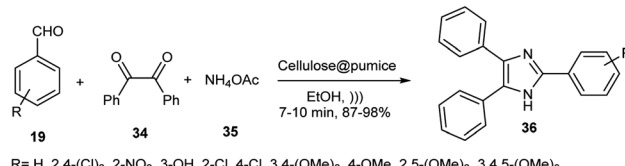


Scheme 3 Synthesis of $\text{Fe}_3\text{O}_4@$ NCS/Sb(v).

Scheme 5 Synthesis of $\text{Fe}_3\text{O}_4@\text{NFC}@\text{Co}(\text{II})$ 26.Scheme 6 Synthesis of 4H-pyrans 27 in the presence of $\text{Fe}_3\text{O}_4@\text{NFC}@\text{Co}(\text{II})$.Scheme 7 Synthesis of pyranopyrazole derivatives 29 using $\text{Fe}_3\text{O}_4@\text{NFC}@\text{Co}(\text{II})$.

advantages of this method are its excellent yields, simple workup, and eco-friendly catalyst. This reaction was accomplished in H_2O : EtOH under reflux conditions in the presence of Fe_3O_4 with 60% yield; however, $\text{Fe}_3\text{O}_4@\text{NCS-PA}$ performed better than Fe_3O_4 in this reaction.⁵⁹

2.1.10. Synthesis and application of $\text{Fe}_3\text{O}_4@\text{NCS/Cu}(\text{II})$. Fe_3O_4 was functionalized with nano-cellulose 5 to obtain



Scheme 9 Synthesis of 2,4,5-triarylimidazoles derivatives 36.

$\text{Fe}_3\text{O}_4@\text{NCs}$ 8, which was added to NaOH solution to give $\text{Fe}_3\text{O}_4@\text{NCs}$ 8, followed by reaction with CuCl_2 to provide $\text{Fe}_3\text{O}_4@\text{NCs/Cu}(\text{II})$ 86 (Scheme 22).⁶⁰

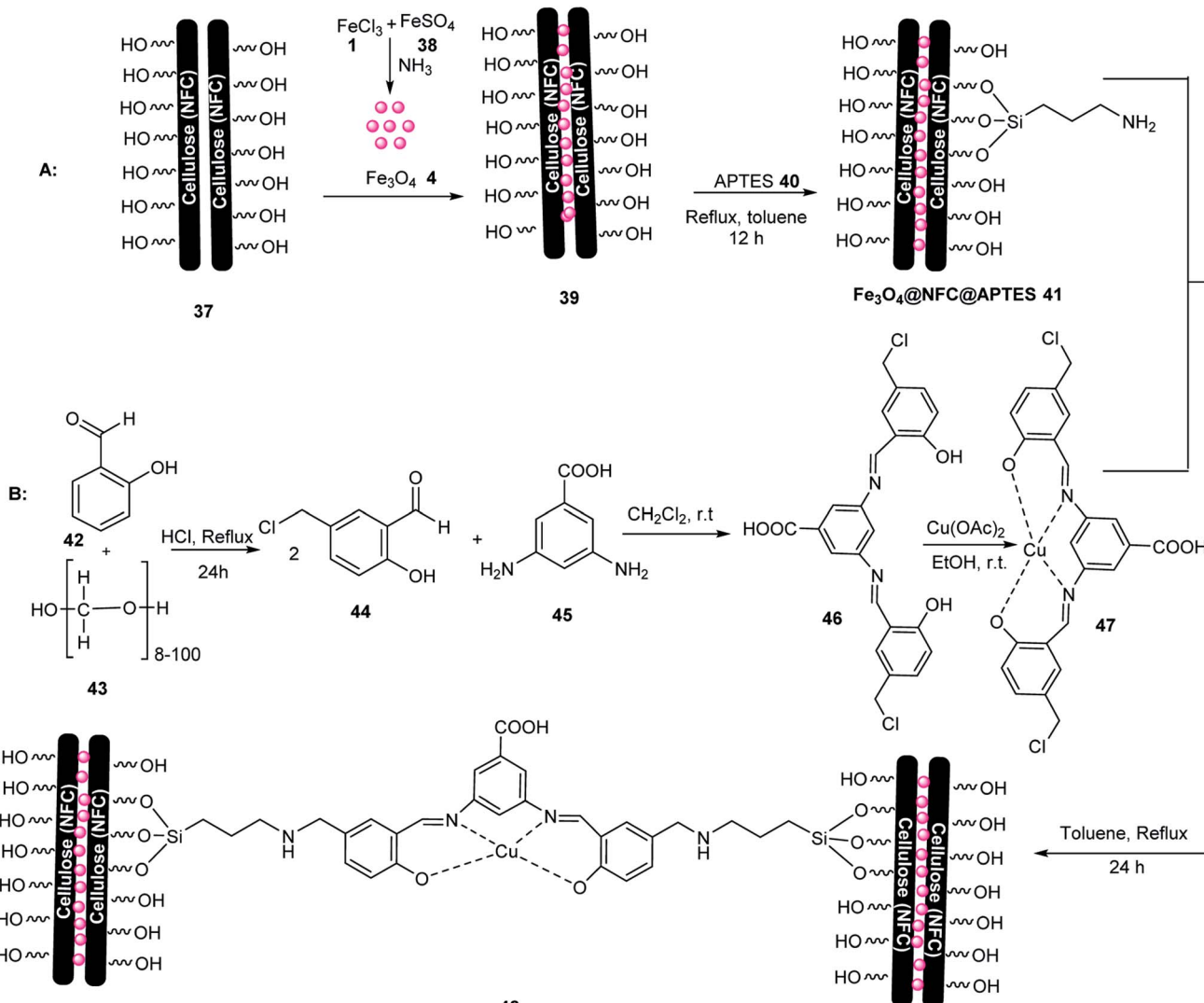
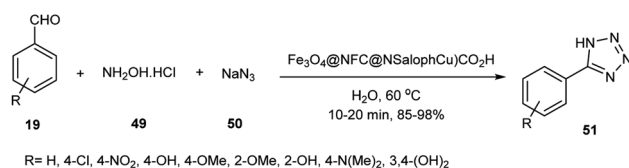
$\text{Fe}_3\text{O}_4@\text{NCs/Cu}(\text{II})$ as a Lewis acid activated the carbonyl groups of the starting materials by copper metal in the synthesis of indenopyrido[2,3-*d*]pyrimidines 89 through the three-component reaction of 6-amino-2-(methylthio)pyrimidin-4(3*H*)-one 88, 1,3-indanedione 87 and aldehydes 19 in EtOH (Scheme 23). The activity of the catalyst was preserved after four runs.⁶⁰

2.1.11. Synthesis and application of $\text{Fe}_3\text{O}_4@\text{nano-cellulose/Cu}(\text{II})$. The reaction of nano-cellulose 5, $\text{FeCl}_3 \cdot 6\text{H}_2\text{O}$, $\text{FeCl}_2 \cdot 4\text{H}_2\text{O}$, and NH_4OH at 80 °C gave $\text{Fe}_3\text{O}_4@\text{nano-cellulose}$ 8, which was reacted with CuCl_2 using sodium hydroxide at room temperature to obtain $\text{Fe}_3\text{O}_4@\text{nano-cellulose/Cu}(\text{II})$ 90 (Scheme 24).⁶¹

$\text{Cu}(\text{II})$ in $\text{Fe}_3\text{O}_4@\text{nanocellulose/Cu}(\text{II})$, as a Lewis acid, activated the carbonyl groups in the three-component reaction of



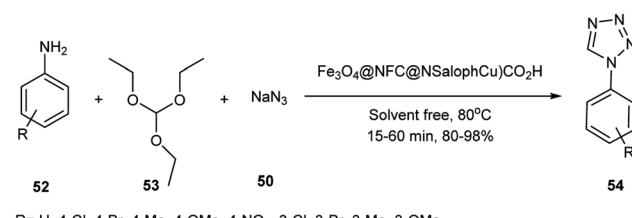
Scheme 8 Synthesis of cellulose@pumice 33.

Scheme 10 Synthesis of $(\text{Fe}_3\text{O}_4@\text{NFC@NSalophCu})\text{CO}_2\text{H}$.Scheme 11 Synthesis of 5-substituted-1*H*-tetrazole 47 using $(\text{Fe}_3\text{O}_4@\text{NFC@NSalophCu})\text{CO}_2\text{H}$.

aromatic aldehydes **19**, 2-aminobenzothiazole **20**, and ethyl acetoacetate **21** for the synthesis of 4*H*-pyrimido[2,1-*b*]benzothiazoles **22** (Scheme 25). The catalyst activity of $\text{Fe}_3\text{O}_4@\text{nano-cellulose/Cu(II)}$ was preserved after four runs. The yield of this reaction in the presence of Fe_3O_4 as a catalyst after 3 h was reported to be about 37%. Therefore, $\text{Fe}_3\text{O}_4@\text{nano-cellulose/Cu(II)}$ is more active than Fe_3O_4 .⁶¹

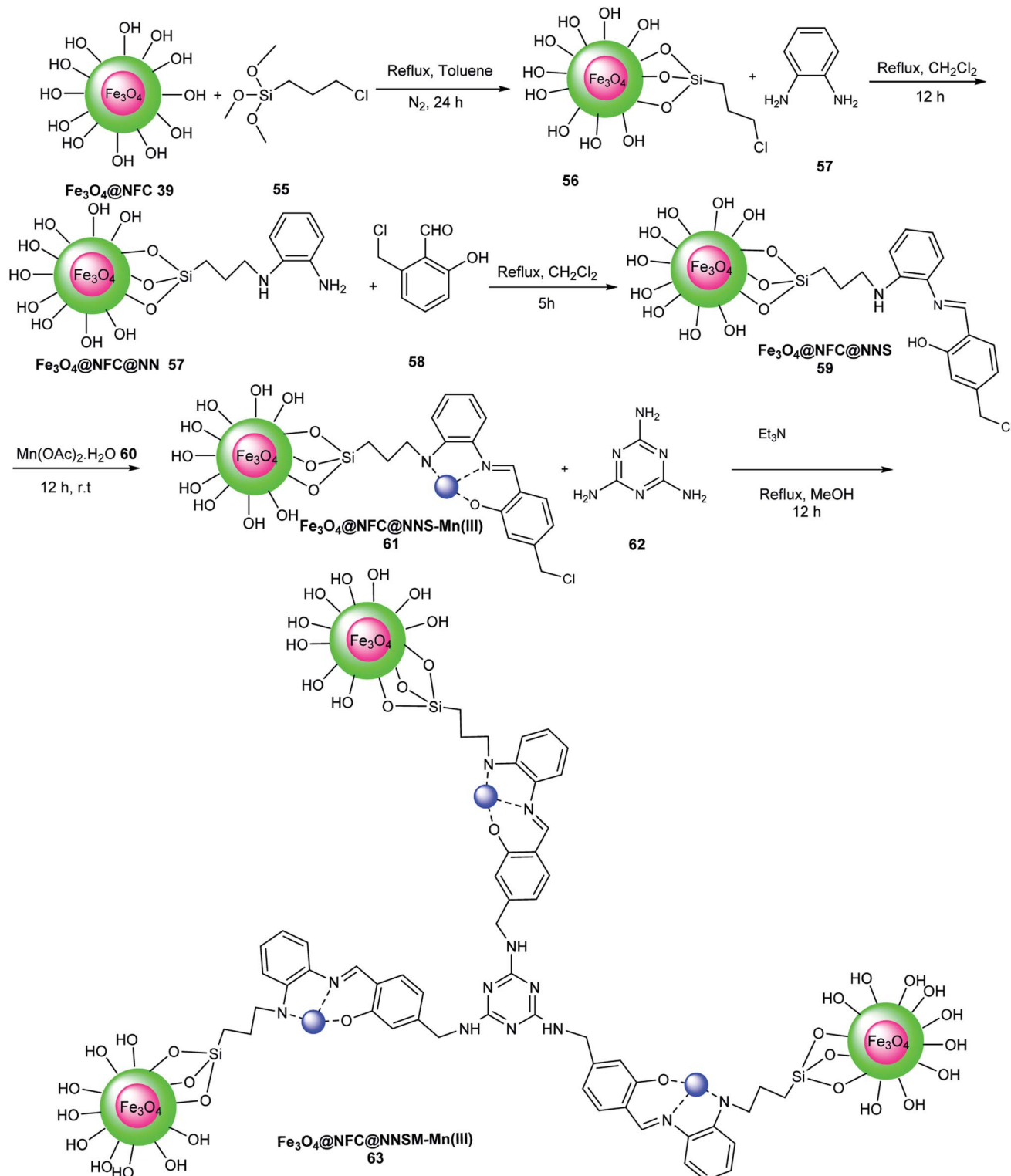
2.1.12. Synthesis and application of $\text{Fe}_3\text{O}_4@\text{NFC-ImSalophCu(II)}$.

Initially, imidazole **11** was treated with 3-

Scheme 12 Synthesis of 1-substituted-1*H*-tetrazoles using $(\text{Fe}_3\text{O}_4@\text{NFC@NSalophCu})\text{CO}_2\text{H}$.

chloropropyl-trimethoxy silane **55** in toluene to produce imidazole-propyl-trimethoxy silane **91**, which was immobilized on $\text{Fe}_3\text{O}_4@\text{NFC}$ using Et₃N as a catalyst in dry toluene to give $\text{Fe}_3\text{O}_4@\text{NFC-Im}$ **92**. The reaction of salicylaldehyde **42** and paraformaldehyde **43** in the presence of HCl/H₂SO₄ gave 5-(chloromethyl)-2-hydroxybenz aldehyde **44**, which was reacted with 1,2-phenylenediamine **93** in dichloromethane under reflux

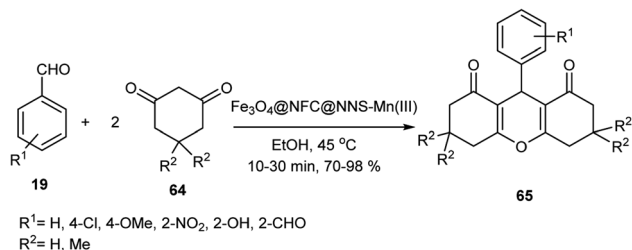


Scheme 13 Synthesis of $\text{Fe}_3\text{O}_4@\text{NFC}@\text{NNSM-Mn(III)}$.

conditions to produce *N,N*-bis(5-chloromethylsalicylidene)-1,2-phenylenediamine 94, followed by reaction with $\text{Cu}(\text{OAc})_2$ in EtOH at room temperature to prepare 5-Cl-Salophen-Cu(II) 95. Finally, $\text{Fe}_3\text{O}_4@\text{NFC-ImSalophCu(II)}$ 96 was synthesized via the

reaction of $\text{Fe}_3\text{O}_4@\text{NFC-Im}$ 92 and 5-Cl-Salophen-Cu(II) 95 in toluene under reflux conditions (Scheme 26).⁶²

The copper of $\text{Fe}_3\text{O}_4@\text{NFC-ImSalophCu(II)}$ 96 was applied in the click reaction of phenacyl bromides 97, sodium azide 90,



Scheme 14 Synthesis of xanthene derivatives **65** in the presence of $\text{Fe}_3\text{O}_4@\text{NFC@NNSM-Mn(III)}$.

and alkynes **98** in H_2O to synthesize 1,2,3-triazoles **99** (Scheme 27). The reusability of this catalyst was tested in the click reaction four times without loss in its activity.⁶²

2.1.13. Synthesis and application of $\text{Fe}_3\text{O}_4@\text{walnut shell/Cu(II)}$. Nanomagnetic $\text{Fe}_3\text{O}_4@\text{walnut shell/Cu(II)}$ was prepared by Mirjalili's research group. Nanomagnetic $\text{Fe}_3\text{O}_4@\text{walnut shell/Cu(II)}$ **100** was prepared *via* the reaction of dried powdered walnut shell with NaOH, hypochlorite solution, and sulfuric acid aqueous to afford a nano walnut shell, followed by reaction with CH_3COOH , $\text{FeCl}_3 \cdot 6\text{H}_2\text{O}$ **1**, $\text{FeCl}_2 \cdot 4\text{H}_2\text{O}_2$, and NH_4OH to generate nanomagnetic $\text{Fe}_3\text{O}_4@\text{walnut shell}$ **8**, which was modified by $\text{CuCl}_2 \cdot 2\text{H}_2\text{O}/\text{NaOH}$ to produce nanomagnetic $\text{Fe}_3\text{O}_4@\text{walnut shell/Cu(II)}$ **100** (Scheme 28).⁶³

Its catalytic activity was explored using 2-aryl/alkyl-2,3-dihydro-1*H*-naphtho[1,2-*e*][1,3]oxazines **102** or **104** or **106** *via* the pseudo-three-component reaction of β -naphthol **101** or α -naphthol **103** or phenol derivatives **105**, formaldehyde **52**, and various amines **43** (Scheme 29). The catalytic activity of nano- $\text{Fe}_3\text{O}_4@\text{walnut shell/Cu}$ did not decrease after five-times use. The copper metal on the nano- $\text{Fe}_3\text{O}_4@\text{walnut shell/Cu(II)}$ increased the reaction rate *via* interaction with the carbonyl group of the starting materials.⁶³

2.2. Magnetic bio-polymers based on dextrin

2.2.1. Synthesis and application of magnetic dextrin nanocomposite. Dextrin **107** is a water-soluble polysaccharide obtained *via* the hydrolysis of starch and glycogen. Magnetic dextrin nanocomposite **108** was prepared *via* the addition of dextrin **107** to a solution of $\text{FeCl}_3 \cdot 6\text{H}_2\text{O}$, $\text{FeCl}_2 \cdot 4\text{H}_2\text{O}$, and ammonium hydroxide at $90\text{ }^\circ\text{C}$ under an N_2 atmosphere *via* the co-precipitation method (Scheme 30).⁶⁴

The magnetic dextrin was tested as a catalyst in the synthesis of polyhydroquinolines *via* four-component reactions of aromatic aldehydes **19**, ethyl acetoacetate **21**, dimedone **61**, ammonium acetate **71** in EtOH under reflux conditions (Scheme 31). The yield of the products did not decrease after five runs. This reaction was performed in the presence of dextrin in ethanol in 28% yield, and thus magnetic dextrin is better than dextrin to catalyze this reaction.⁶⁴

2.2.2. Synthesis and application of magnetized dextrin. Magnetized dextrin **72** was obtained *via* the reaction of $\text{FeCl}_3 \cdot 6\text{H}_2\text{O}$, $\text{FeCl}_2 \cdot 4\text{H}_2\text{O}$, dextrin **71**, and NH_4OH in H_2O at $90\text{ }^\circ\text{C}$ under a nitrogen atmosphere (Scheme 32).⁶⁵

Maleki *et al.* studied the catalytic activity of magnetized dextrin **29** for the synthesis of dihydropyrano[2,3-*c*]pyrazoles **29** through the reaction of hydrazine hydrate **28**, ethyl acetoacetate **21**, aromatic aldehydes **19**, and malononitrile **14** under reflux conditions in EtOH (Scheme 33). This catalyst was used for five runs without a decrease in its catalytic activity.⁶⁵

2.2.3. Synthesis and application of FND-Ti(IV) . $\text{Fe}_3\text{O}_4@\text{nano-dextrin}$ **108** was prepared through the reaction of nano-dextrin **107**, $\text{FeCl}_3 \cdot 6\text{H}_2\text{O}$, $\text{FeCl}_2 \cdot 4\text{H}_2\text{O}$, and ammonia solution in H_2O at $80\text{ }^\circ\text{C}$. $\text{Fe}_3\text{O}_4@\text{nano-dextrin}$ **108** was coated with TiCl_4 in CH_2Cl_2 to prepare FND-Ti(IV) **109** (Scheme 34).⁶⁶

Its catalytic activity as a Lewis acid was investigated in the synthesis of 2,3-dihydroquinazolin-4(*H*)-ones **85** *via* the condensation reaction of 2-aminobenzamide **84** and aldehydes **19** under mild conditions (Scheme 35). This catalyst was used five times without loss in its catalytic activity.⁶⁶

2.3. Magnetic bio-polymers based on starch

2.3.1. Synthesis and application of magnetic $\text{Ag/Fe}_3\text{O}_4@\text{starch}$ nanocatalyst. To aqueous starch solution **110**, citric acid **111** and sodium hypophosphite **112** were added and refluxed to give the precipitate crude product, which was crushed and dried to give cross-linked starch **113**, followed by dissolving in H_2O to produce gelatinized starch **114**. The obtained gelatinized starch was reacted with $\text{FeCl}_3 \cdot 6\text{H}_2\text{O}$, and $\text{FeSO}_4 \cdot 7\text{H}_2\text{O}$ in H_2O at room temperature, and then mixed with NH_3 dropwise to give the $\text{Fe}_3\text{O}_4@\text{starch}$ nanocatalyst, which was treated with AgNO_3 (aq) to generate the magnetic $\text{Ag/Fe}_3\text{O}_4@\text{starch}$ **115** nanocatalyst (Scheme 36).⁶⁷

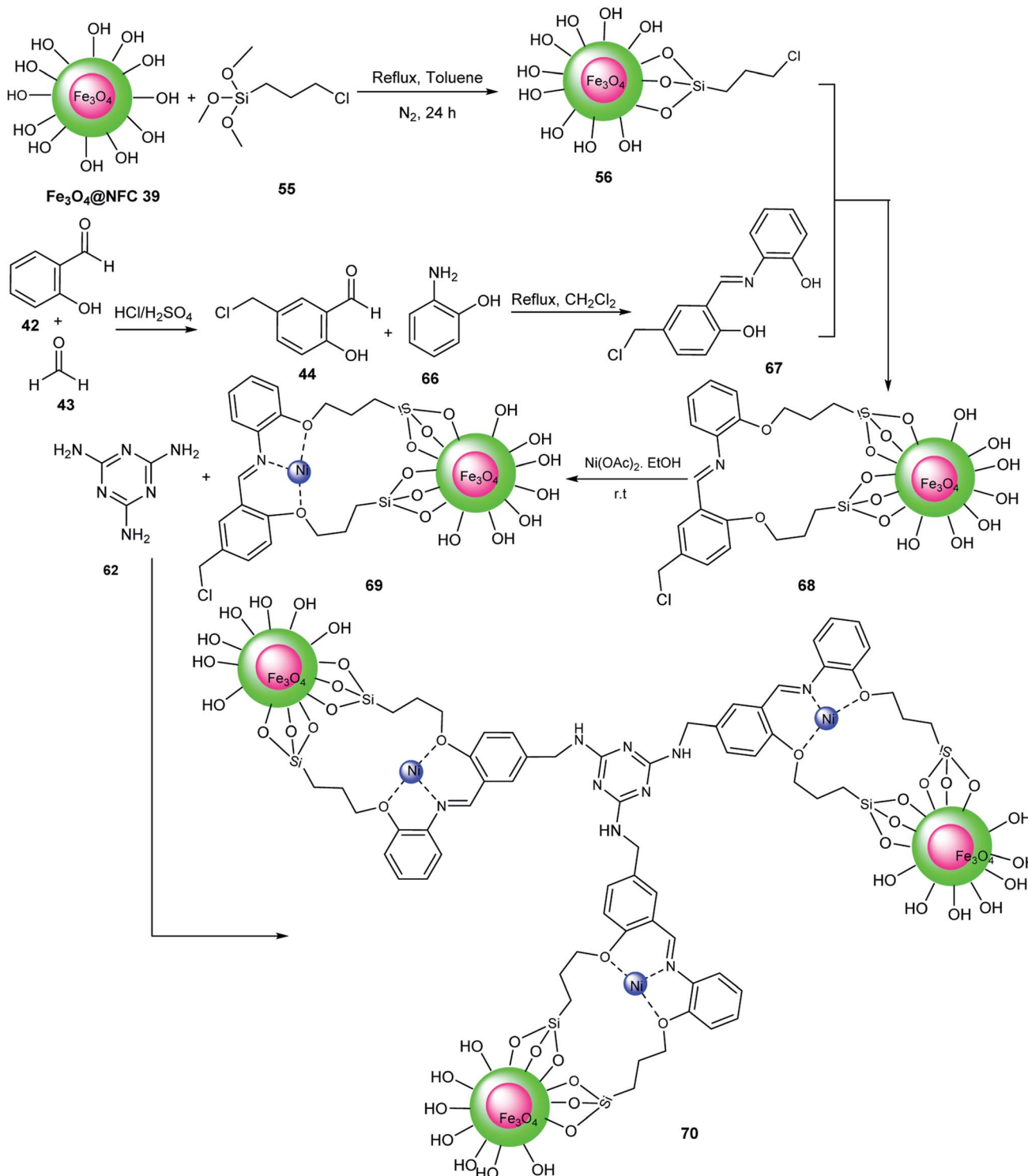
The catalytic activity of $\text{Ag/Fe}_3\text{O}_4@\text{starch}$ as Lewis acid **115** was evaluated in the one-pot reaction of benzaldehydes **19**, malononitrile **14**, and dimedone **64** in EtOH for the synthesis of 4*H*-pyran **116** (Scheme 37). Also, the magnetic nanocatalyst was reused five times with no loss in its activities.⁶⁷

2.3.2. Synthesis and application of magnetic $\text{CuFe}_2\text{O}_4@\text{starch}$. To obtain $\text{CuFe}_2\text{O}_4@\text{starch}$ **122**, $\text{Cu}(\text{NO}_3)_2$ **117** was reacted with $\text{Fe}(\text{NO}_3)_3$ **118** using sodium hydroxide in H_2O to give CuFe_2O_4 nanoparticles **121**, followed by reaction with starch to obtain $\text{CuFe}_2\text{O}_4@\text{starch}$ **122**. Its catalytic activity was tested in the synthesis of 4*H*-chromene **125** or **126** *via* the three-component reaction of various aldehydes **19**, malononitrile **14**, 2-hydroxy-1,4-naphthoquinone **123**, or 4-hydroxycoumarin **124** (Scheme 38).⁶⁸

In another attempt, 2-amino-5-oxo-5,6,7,8-tetrahydro-4*H*-benzo[*b*]pyrans **27** or **116** were synthesized *via* the reaction of aldehydes **19**, malononitrile **14**, and enolizable C-H-activated acidic compounds, including dimedone **64** and ethyl acetoacetate **21**, in the presence of $\text{CuFe}_2\text{O}_4@\text{starch}$ **122** as a Lewis acid in EtOH . The reaction rate for aldehydes with electron-withdrawing groups was faster than that with electron-donating groups (Scheme 39 and 40), respectively. This catalyst was used in six runs without a decrease in its activity.⁶⁸

2.3.3. Synthesis and application of magnetic starch/SPION@ SO_3H . Superparamagnetic iron oxide nanoparticles (SPION) **127** were synthesized *via* the reaction of Fe^{2+} , Fe^{3+} , and ammonia in aqueous media. Then, SPION **127** was coated with



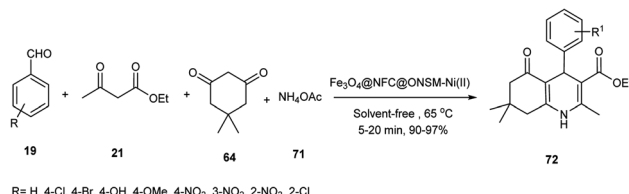
Scheme 15 Synthesis of Fe_3O_4 @NFC@ONSM-Ni(II).

tetraethyl orthosilicate (TEOS) to give SPION@ SiO_2 128, which was reacted with starch 110 to give magnetic starch, followed by reaction with allyltrimethoxysilane 130 to prepare allyl-functionalized magnetic starch 131. Finally, starch/SPION@ SO_3H 133 was synthesized *via* the polymerization of

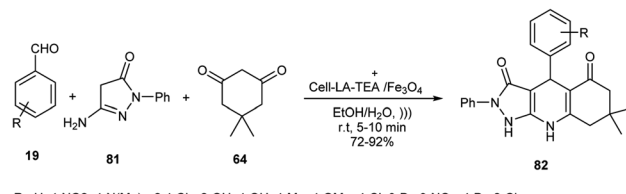
allyl-functionalized magnetic starch 131 and 4-styrenesulfonic acid 132 (Scheme 41).⁶⁹

Starch/SPION@ SO_3H 133 as a Brønsted acid (SO_3H) activated the carbonyl groups in the multicomponent reaction of 4-hydroxycoumarin 124, benzaldehydes 19, dimedone 64, and

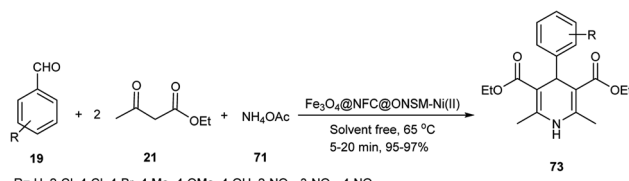




Scheme 16 Synthesis of polyhydroquinolines **72** in the presence of $\text{Fe}_3\text{O}_4@\text{NFC@ONSM-Ni(II)}$.



Scheme 19 Synthesis of pyrazolo quinolones **82** in the presence of Cell-LA-TEA⁺/ Fe_3O_4 .



Scheme 17 Synthesis of 1,4-dihydropyridine **73** in the presence of $\text{Fe}_3\text{O}_4@\text{NFC@ONSM-Ni(II)}$.

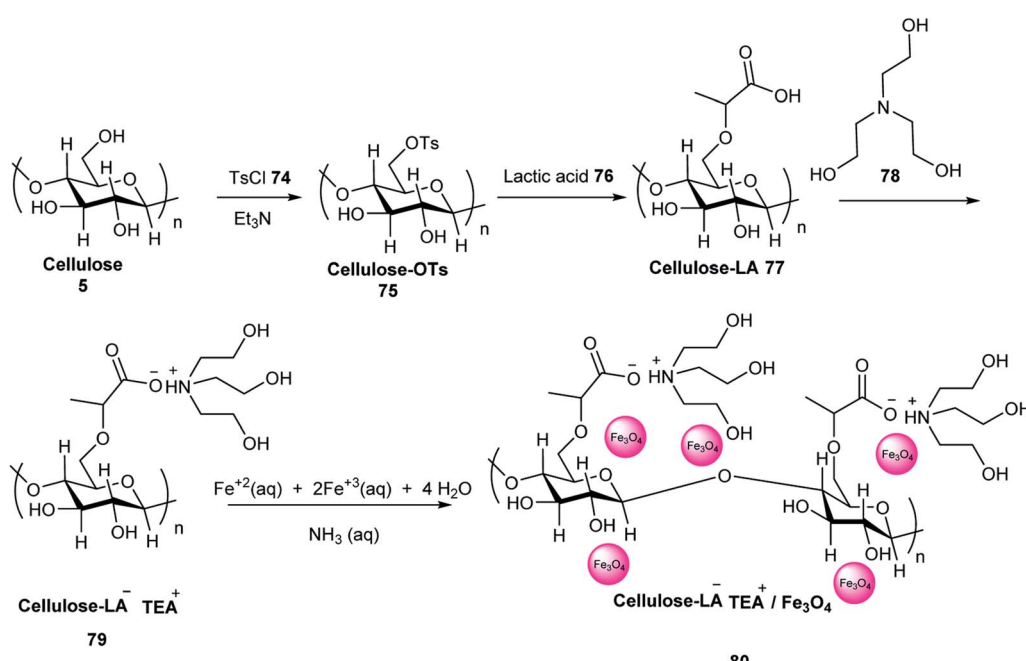
ammonium acetate **71** in the synthesis of chromeno[4,3-*b*]quinoline-6,8(9*H*)-dione derivatives **134** (Scheme 42). This catalyst was applied ten times without any loss in its activity.⁶⁹

2.3.4. Synthesis and application of magnetic $\text{Fe}_3\text{O}_4@\text{GOTfOH/Ag/St-PEG-AcA}$. Initially, through the Hummers' method, graphite **135** was treated with H_2SO_4 , KMnO_4 , and H_2O to give GO **136**, which was treated with FeCl_3 , FeCl_2 , and ammonium solution at 80 °C to achieve $\text{Fe}_3\text{O}_4@\text{GO}$ **137**, followed by reaction with trifluoro methanesulfonic acid in CH_2CH_2 to give $\text{Fe}_3\text{O}_4@\text{GOTfOH}$ **138**. In the next step, starch **139** was dissolved in water at 80 °C. Subsequently, *N,N*-

methylene acrylene acrylamide (MBA) **140** was dissolved in water. Then, the above-mentioned two mixtures were mixed to obtain a homogeneous viscous mixture. Then, a certain amount of acrylic acid **141** and PEG-poly **142** was added to the reaction mixture. Then, ammonium persulfate (APS) **143** solution was added to the reaction mixture until a hydrogel was obtained. The above-mentioned homogeneous solution, AgNP **144** colloidal solution and $\text{Fe}_3\text{O}_4@\text{GOTfOH/Ag/St-PEG-AcA}$ **146** (Scheme 43).⁷⁰

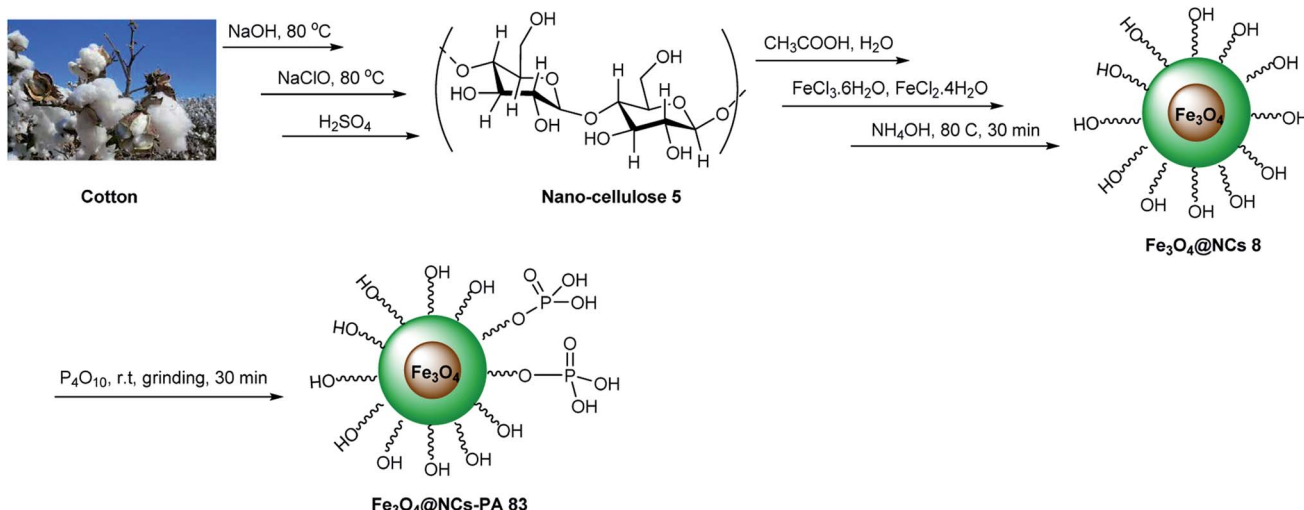
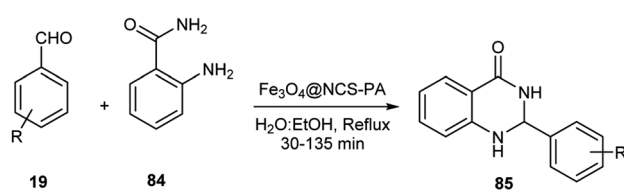
The catalytic activity of $\text{Fe}_3\text{O}_4@\text{GOTfOH/Ag/St-PEG-AcA}$ **146** was examined in the synthesis of 2,4,6-triarylpyridines **137** through the pseudo-three-component reaction of aryl aldehydes **19**, acetophenone **147** and ammonium acetate **71** (Scheme 44). According to the catalyst structure, the carbonyl groups were activated *via* interaction with the Brønsted acid site and Lewis acid of Fe^{3+} . Also, the catalytic activity of **146** did not decrease after 10 runs.⁷⁰

2.3.5. Synthesis and application of magnetic $\gamma\text{-Fe}_3\text{O}_4@\text{starch-}n\text{-butyl SO}_3\text{H}$. Fe_3O_4 nanoparticles **4** were synthesized *via* the reaction of $\text{FeCl}_2 \cdot 4\text{H}_2\text{O}$ **2** and $\text{FeCl}_3 \cdot 6\text{H}_2\text{O}$ **1** and NH_4OH solution in H_2O an under argon atmosphere at room



Scheme 18 Synthesis of Cell-LA-TEA⁺/ Fe_3O_4 .

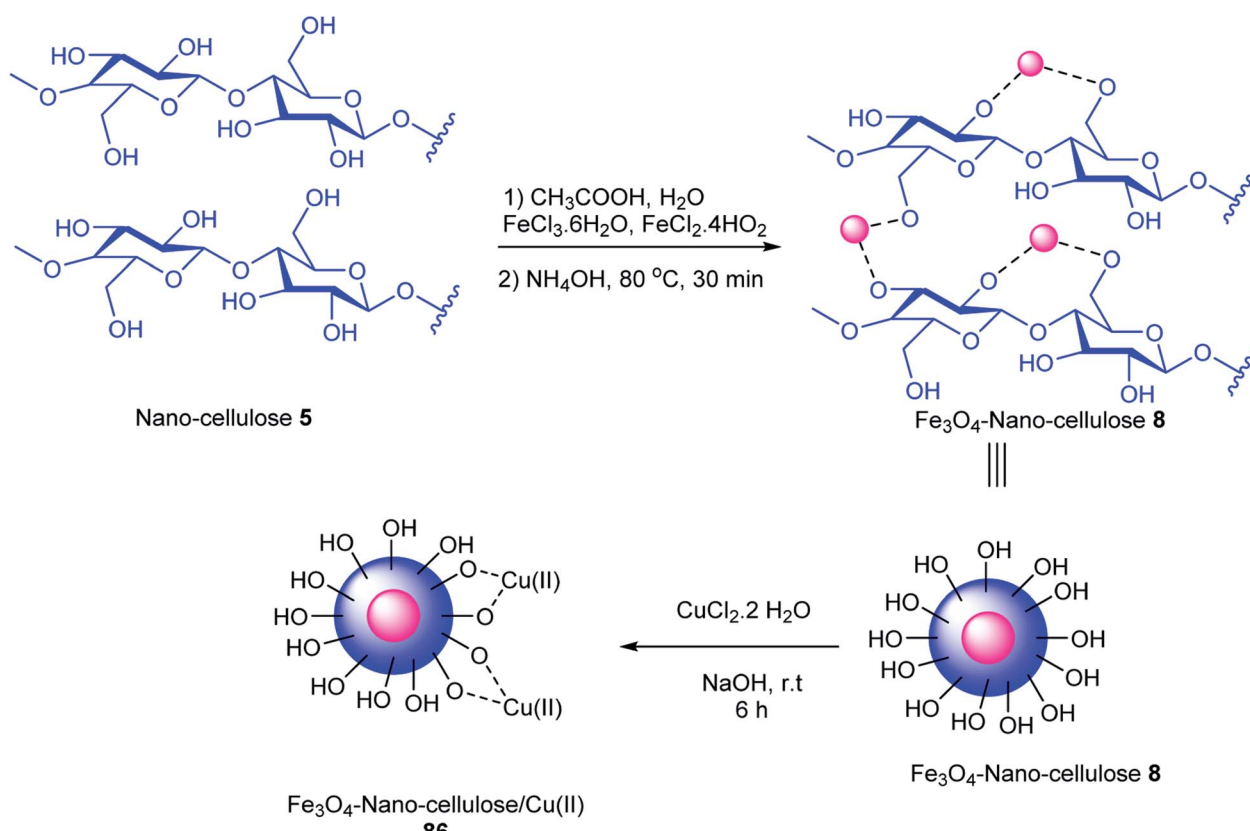


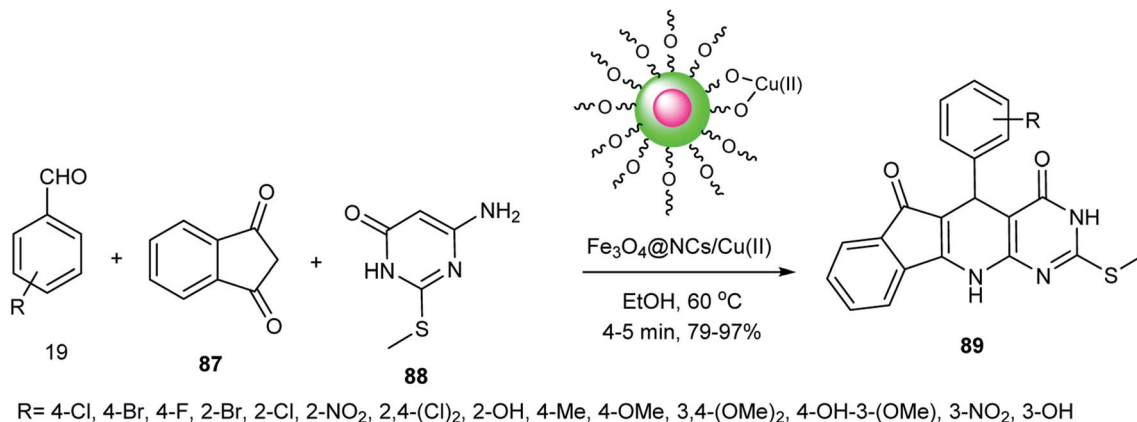
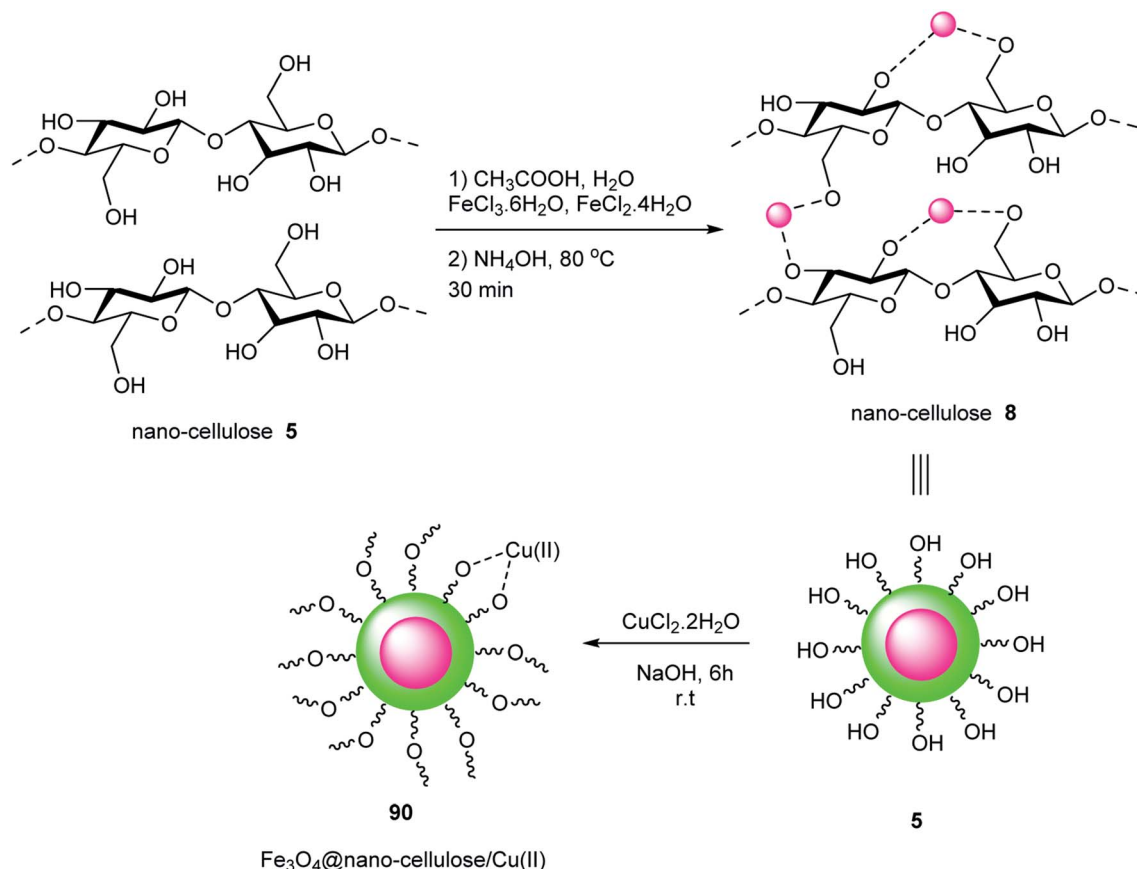
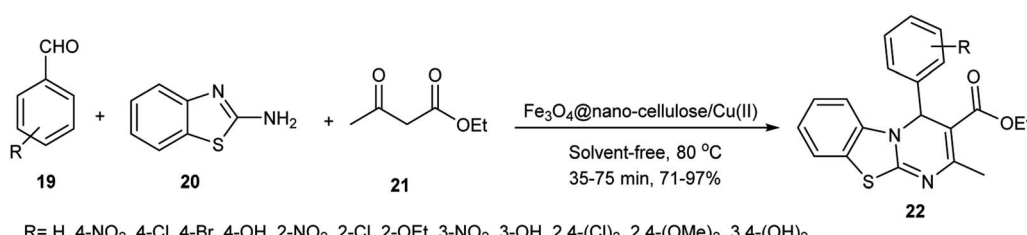
Scheme 20 Synthesis of Fe₃O₄@NCS-PA.

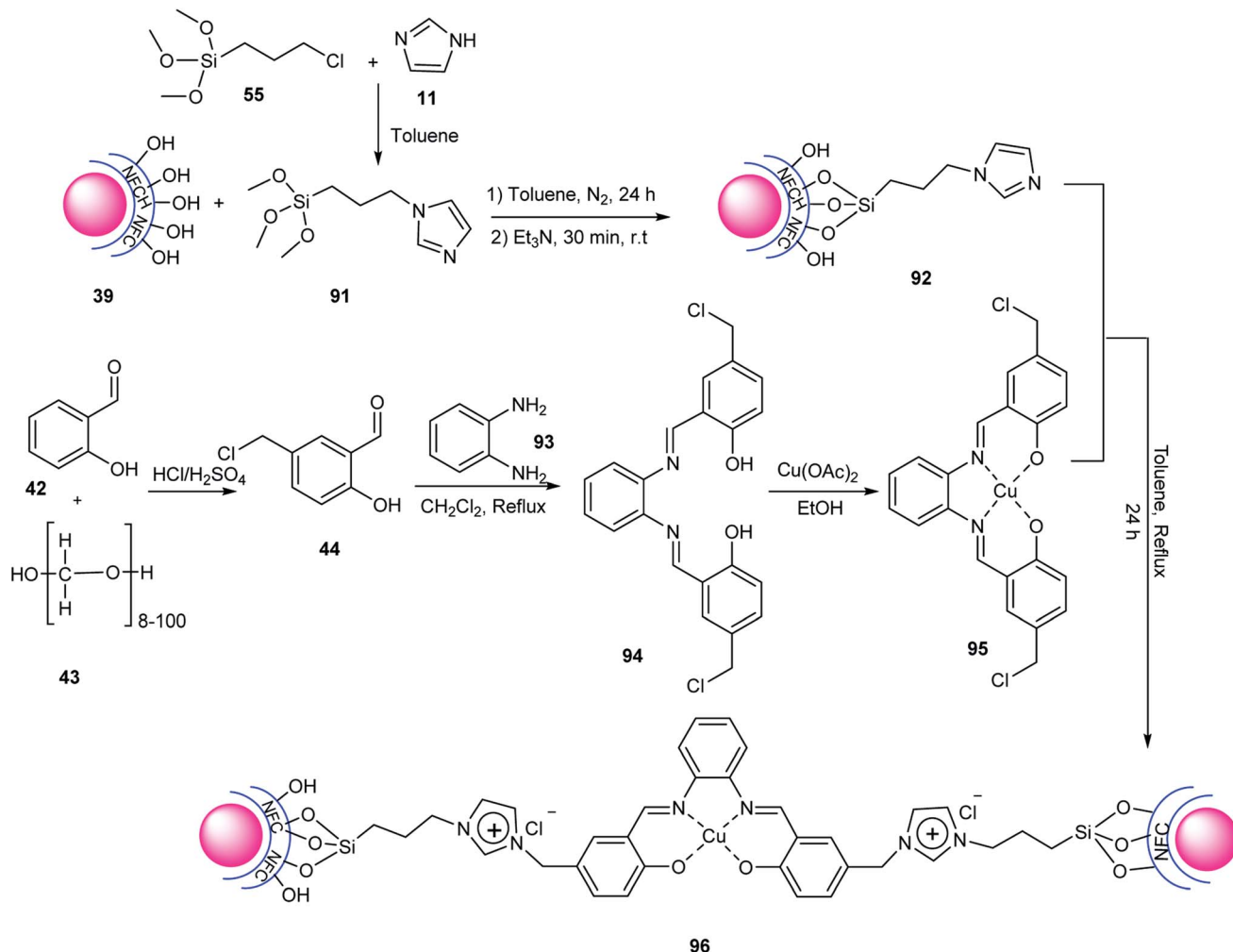
Scheme 21 Synthesis of 2,3-dihydroquinazolin-4(1H)-ones.

temperature. Then, γ -Fe₂O₃ was synthesized using Fe₃O₄ at 250 °C. In the next step, γ -Fe₂O₃ was coated with starch at room temperature to obtain γ -Fe₂O₃@starch **150**, followed by reaction with 1,4-butane sultone **151** in dry toluene under reflux conditions to produce γ -Fe₂O₃@starch-*n*-butylSO₃H **152** nanoparticles (Scheme 45).⁷¹

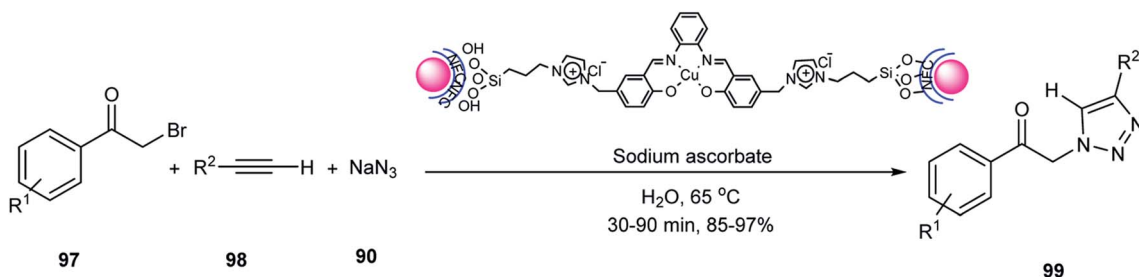
γ -Fe₂O₃@starch-*n*-butylSO₃H **152** as Brønsted acid activated the carbonyl groups in the multicomponent reactions of

Scheme 22 Synthesis of Fe₃O₄@NCs/Cu(II) **86**.

Scheme 23 Synthesis of indenopyrido [2,3-d] pyrimidines in the presence of $\text{Fe}_3\text{O}_4@\text{NCs}/\text{Cu}(\text{II})$.Scheme 24 Synthesis of $\text{Fe}_3\text{O}_4@\text{nano-cellulose}/\text{Cu}(\text{II})$.Scheme 25 Synthesis of 4H-pyrimido[2,1-b]benzothiazole derivatives 22 using $\text{Fe}_3\text{O}_4@\text{nano-cellulose}/\text{Cu}(\text{II})$.



Scheme 26 Synthesis of 4H-pyrimido[2,1-*b*]benzothiazole derivatives using $\text{Fe}_3\text{O}_4@\text{NFC-ImSalophCu(II)}$ 96.



Scheme 27 Synthesis of 1,2,3-triazoles 99 using $\text{Fe}_3\text{O}_4@\text{NFC-ImSalophCu}$.

aldehydes **19**, dimedone **64**, and 2-aminobenzimidazole **153** or phthalhydrazide **154** to synthesize tetrahydrobenzimidazo[2,1-*b*]quinazolin-1(2*H*)-ones **155** or 2*H*-indazolo[2,1-*b*]phthalazine-trione **156** (Scheme 46). This catalyst was used seven times without loss in any of its activities.⁷¹

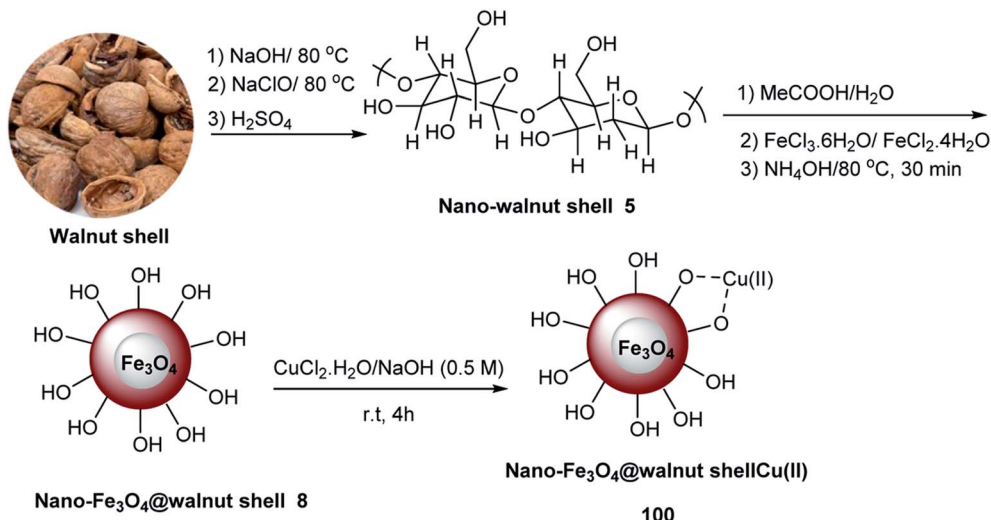
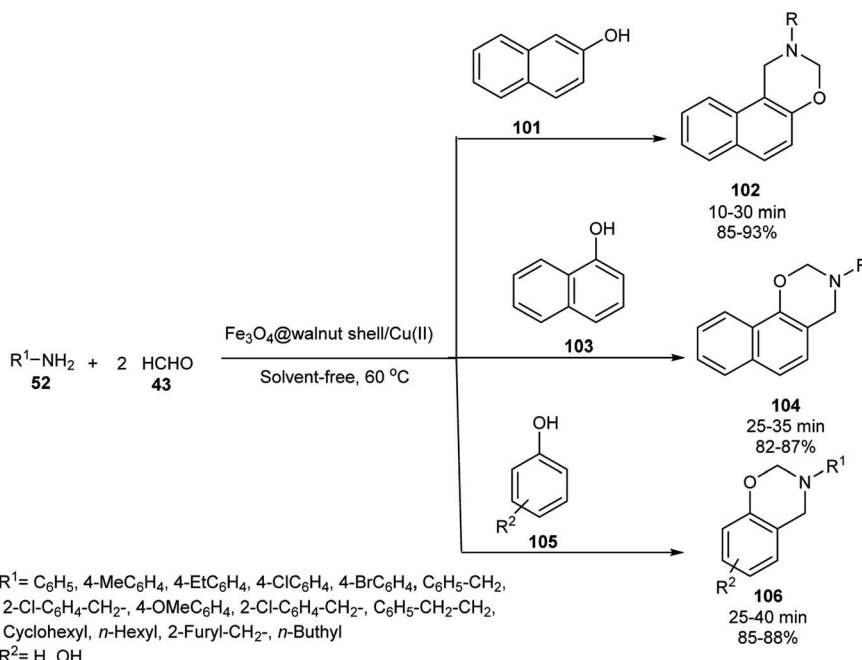
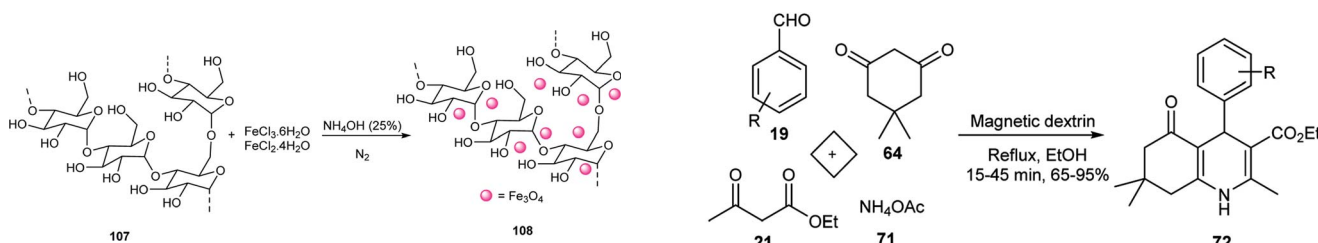
2.4. Magnetic bio-polymers based on alginate

2.4.1. Synthesis and application of $\text{Fe}_3\text{O}_4@\text{Alg}@{\text{CPTMS}}$

Alg@CPTMS@Arg. Alginate **157** was immobilized on Fe_3O_4 **4** via

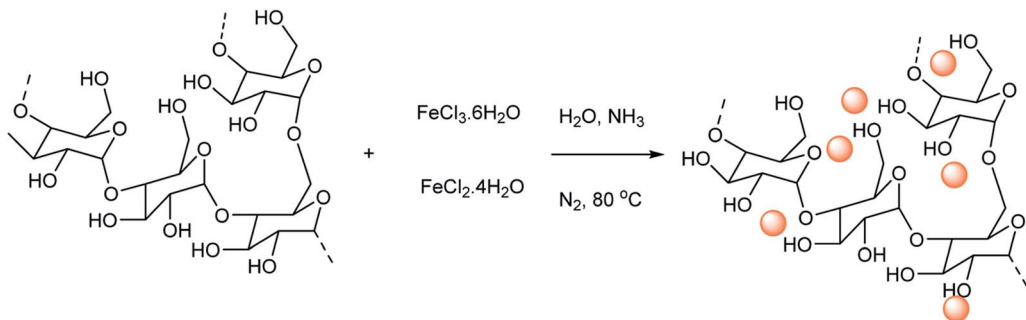
the co-precipitation method. Initially, $\text{FeCl}_3 \cdot 6\text{H}_2\text{O}$ **1**, $\text{FeCl}_2 \cdot 4\text{H}_2\text{O}$ **2**, and sodium alginate **157** were dissolved in H_2O under a nitrogen atmosphere. Then, an ammonia solution was added to this mixture to give $\text{Fe}_3\text{O}_4@\text{Alg}$ nanoparticles **158**, which were functionalized with 3-chloropropyltrimethoxysilane **55** to prepare $\text{Fe}_3\text{O}_4@\text{Alg}@{\text{CPTMS}}$ **159**, followed by reaction with *L*-arginin **160** using trimethylamine in EtOH for 48 h to give $\text{Fe}_3\text{O}_4@\text{Alg}@{\text{CPTMS}}@\text{Arg}$ **161** (Scheme 47).⁷²



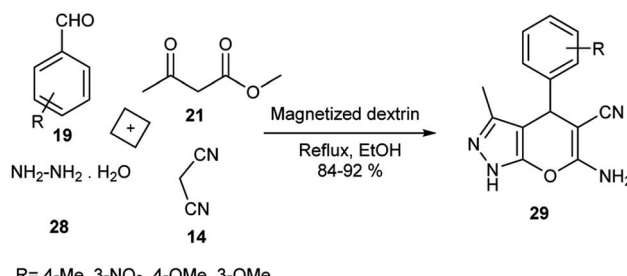
Scheme 28 Synthesis of nano-Fe₃O₄@walnut shell/Cu.Scheme 29 Synthesis of 2-aryl/alkyl-2,3-dihydro-1H-naphtho[1,2-e][1,3]oxazines 102 or 104 or 106 using nano-Fe₃O₄@walnut shell/Cu(II).

Scheme 30 Synthesis of magnetic dextrin.

Scheme 31 Synthesis of polyhydroquinolines 72 in the presence of magnetic dextrin.



Scheme 32 Synthesis of magnetized dextrin.



Scheme 33 Synthesis of dihydropyrano[2,3-c]pyrazoles 29 using magnetized dextrin.

Subsequently, $\text{Fe}_3\text{O}_4@\text{Alg}@\text{CPTMS}@\text{Arg}$, which has two acidic and basic functional sites, activated the carbonyl groups in the synthesis of 2,4,5-triarylimidazoles through the reaction of ammonium acetate, aldehydes, and benzil in EtOH under reflux conditions (Scheme 48). The recyclability of the catalyst

was tested 7 times using the model reaction without loss in any of its activities. When Fe_3O_4 was used as the catalyst, the yield of this reaction was about 65%.⁷²

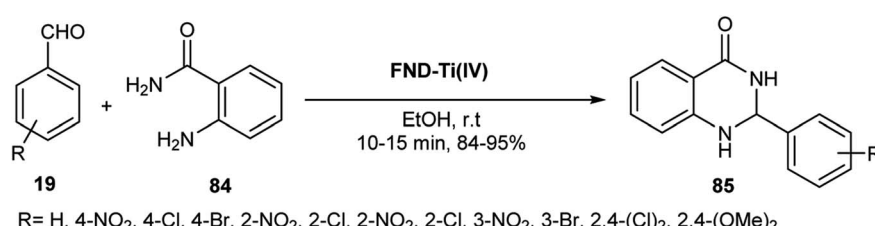
2.4.2. Synthesis and application of $\text{Fe}_3\text{O}_4@\text{Alg}@\text{CPTMS}@\text{Arg}$. The reaction of $\text{Fe}_3\text{O}_4@\text{Alg}$ 165 and 3-chloropropyltrimethoxysilane (CPTMS) 55 in toluene under reflux conditions and nitrogen atmosphere gave $\text{Fe}_3\text{O}_4@\text{Alg}@\text{CPTMS}$ 166, which was reacted with arginine 167 in the presence of trimethylamine in dry toluene to provide $\text{Fe}_3\text{O}_4@\text{Alg}@\text{CPTMS}@\text{Arg}$ nanocomposites 168 (Scheme 49).⁷³

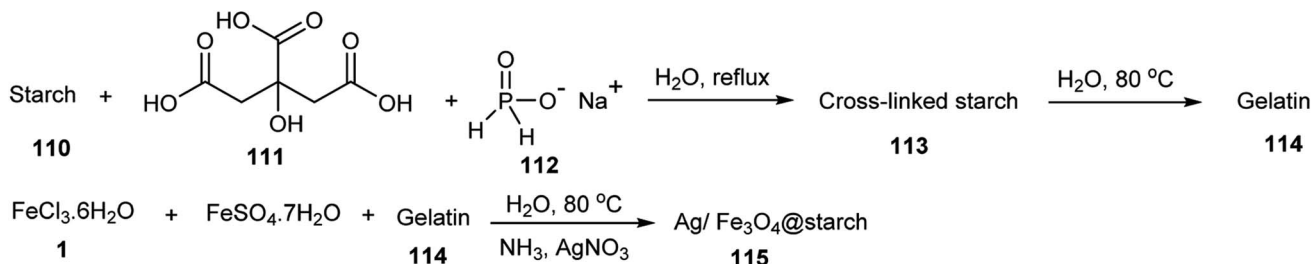
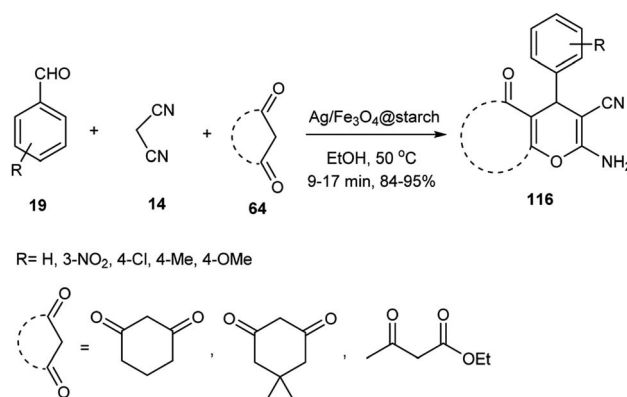
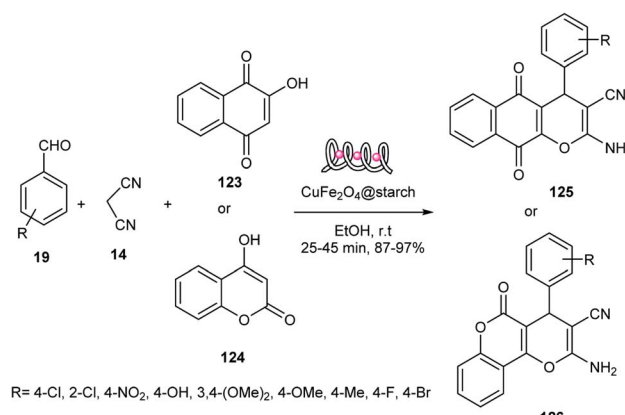
The activity of $\text{Fe}_3\text{O}_4@\text{Alg}@\text{CPTMS}@\text{Arg}$ was tested as a catalyst in the synthesis of 2,4,5-triarylimidazoles 36 *via* the reaction of ammonium acetate 71, aldehyde derivatives 19, and benzil 34 in EtOH (Scheme 50). Its catalytic activity did not decrease after seven uses. It has two functional groups including a Lewis base (NH_2) and Brønsted acidic (COOH), which catalyzed the synthesis of 2,4,5-triarylimidazoles.⁷³

2.4.3. Synthesis and application of $\text{Fe}_3\text{O}_4@\text{FU}$. $\text{Fe}_3\text{O}_4@\text{FU}$ 170 was prepared *via* the reaction of fucoidan powder 169,



Scheme 34 Synthesis of FND-Ti(IV) 109.

Scheme 35 Synthesis of 2,3-dihydroquinazolin-4(1H)-ones 85 using $\text{Fe}_3\text{O}_4@\text{nano-dextrin}/\text{Ti}(\text{IV})$.

Scheme 36 Synthesis of Ag/Fe₃O₄@starch 115.Scheme 37 Synthesis of 4H-pyran 116 in the presence of Ag/Fe₃O₄@starch.Scheme 39 Synthesis of 4H-chromenes using CuFe₂O₄@starch.

FeCl₂·4H₂O 2, and FeCl₃·6H₂O 1 in aqueous ammonia solution (25%) in distilled water under a nitrogen atmosphere at 80 °C (Scheme 51).⁷⁴

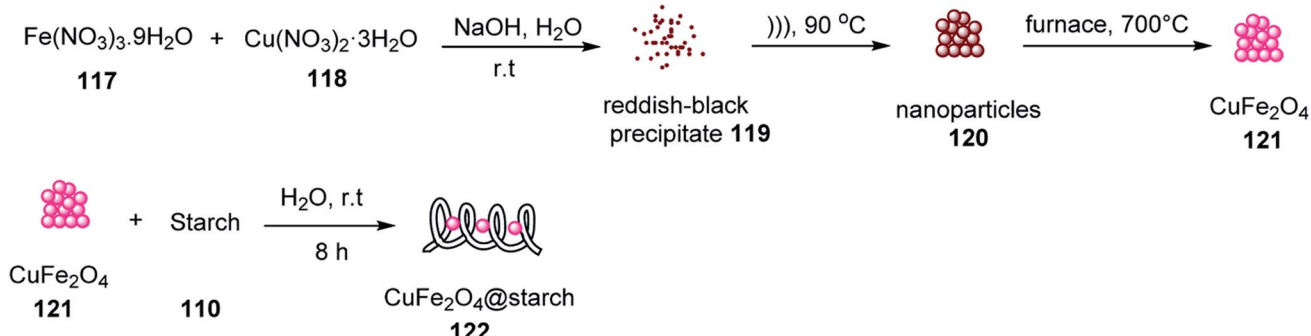
The activity of Fe₃O₄@FU was evaluated as a catalyst in the synthesis of *tri*- and *tetra*-substituted imidazoles 36 or 171 *via* three- and four-component reactions of benzil 34, aldehydes 19, NH₄OAc 71, and amine 52 under reflux conditions in EtOH (Scheme 52), respectively. The catalyst was used six times in the model reaction without loss in any of its activities. This reaction was accomplished in ethanol under reflux conditions in the presence of Fe₃O₄ as a catalyst after 40 min with 55% yield. The carbonyl groups were activated *via* hydrogen bonding with Fe₃O₄@FU as a catalyst.⁷⁴

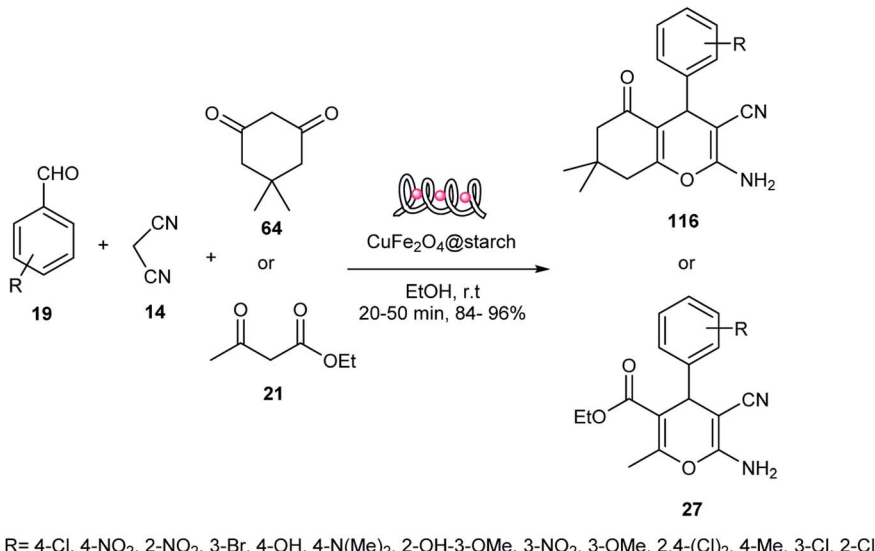
2.5. Magnetic bio-polymers based on glucose

2.5.1. Synthesis and application of Fe₃O₄@C@ONa.

Initially, FeCl₃·6H₂O solution, CO(NH₂)₂, and glucose were added to ethylene glycol 172 to produce a black powder of carbon-coated magnetic nanoparticles (CCMNPs: Fe₃O₄@C) 173, followed by reaction with NaOH solution to obtain basic carbon-coated magnetic nanoparticles (BCCMNs: Fe₃O₄@C@ONa) 174 (Scheme 53).⁷⁵

Subsequently, the catalytic activity of Fe₃O₄@C@ONa was tested for the synthesis of 4H-chromene derivatives 174 *via* the reaction of salicylaldehyde 42, dimedone 64, and β-naphthol 101 in water at 60 °C (Scheme 54). Also, the catalyst was used five times in the model reaction without loss in any of its

Scheme 38 Synthesis of CuFe₂O₄@starch.



Scheme 40 Synthesis of 2-amino-5-oxo-5,6,7,8-tetrahydro-4H-benzo[b]pyrans 116 or 27.

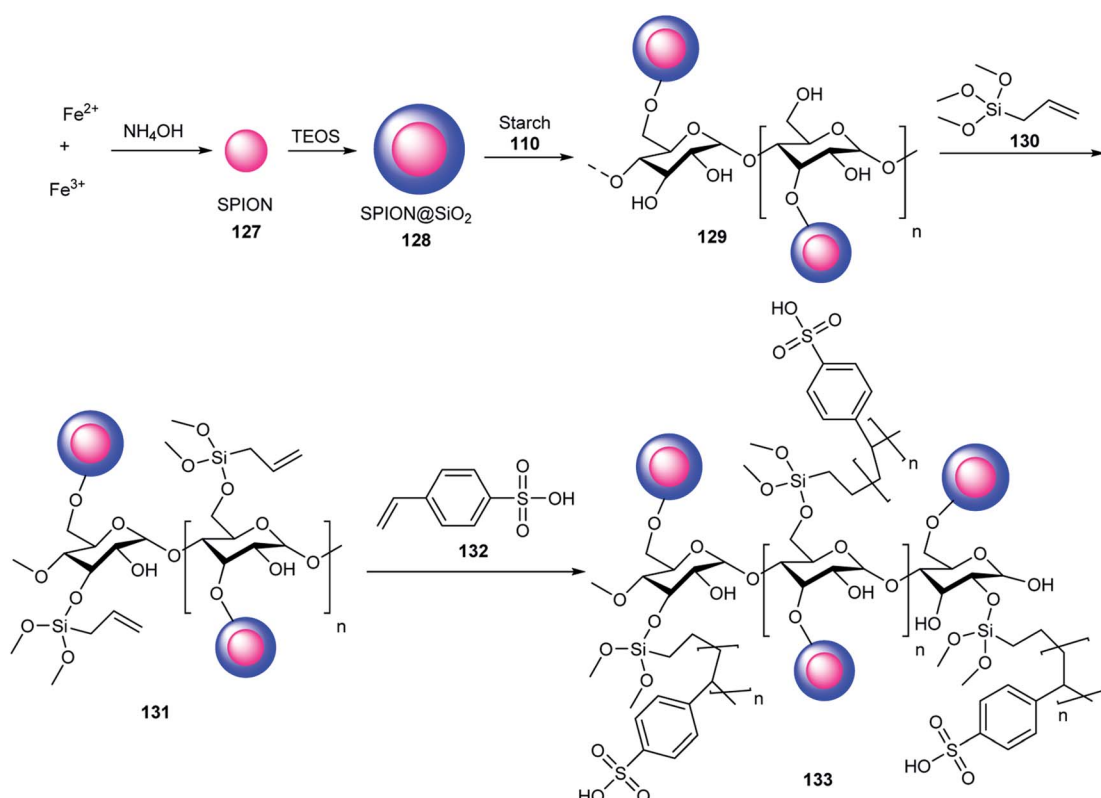
activities. This catalyst has two functional groups, including Fe³⁺ as a Lewis acid and oxygen group as a Lewis base, which increased the reaction rate.⁷⁵

2.6. Magnetic bio-polymers based on chitosan

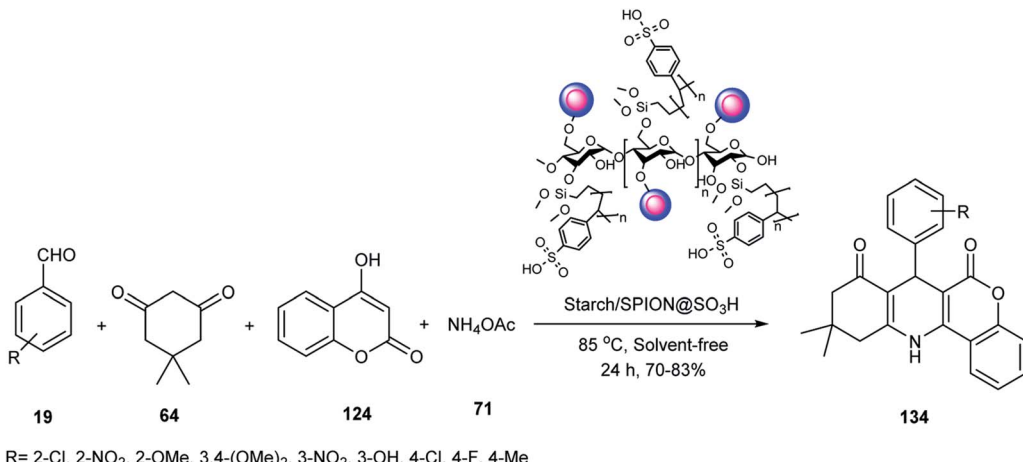
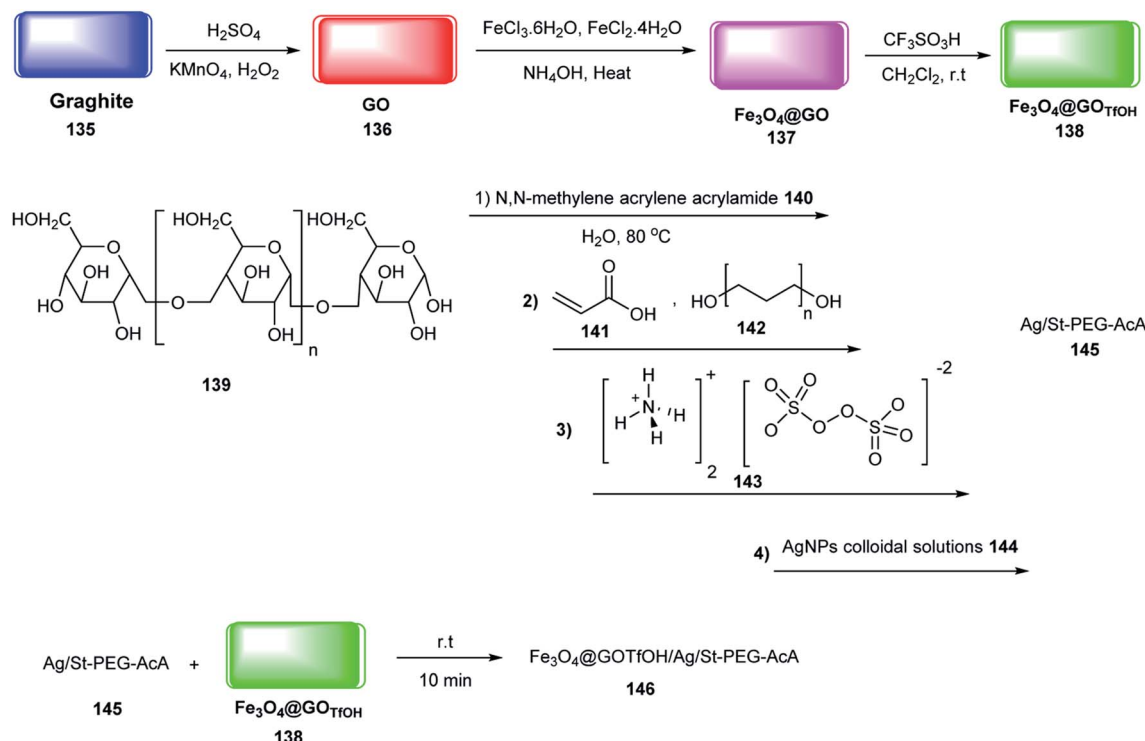
2.6.1. Synthesis and application of CSSNH@Arg. Chitosan-silica sulfate nanohybrid (CSSNH@Arg) 178 was synthesized *via*

the reaction of chitosan 176 and silica sulfuric acid (SSA) 177 under ultrasonic irradiation (Scheme 55).⁷⁶

A green method for the synthesis of 3,4-dihydropyrimidine-2(1H)-one/thione derivatives 179 was described by Behrouz and co-workers *via* the Biginelli reaction of (thio)urea 23 or urea 6, methyl acetoacetate 21, and aldehydes 19 using CSSNH@Arg 178 under solvent-free conditions (Scheme 56).



Scheme 41 Synthesis of starch/SPION@SO₃H.

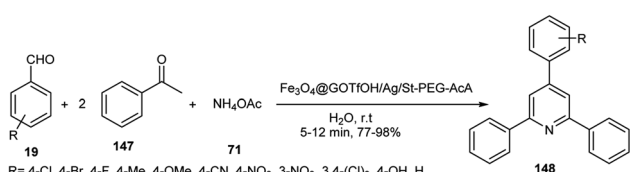
Scheme 42 Synthesis of chromeno[4,3-b]quinoline-6,8(9H)-diones in the presence of Starch/SPION@SO₃H.Scheme 43 Synthesis of Fe₃O₄@GOTfOH/Ag/St-PEG-AcA 146.

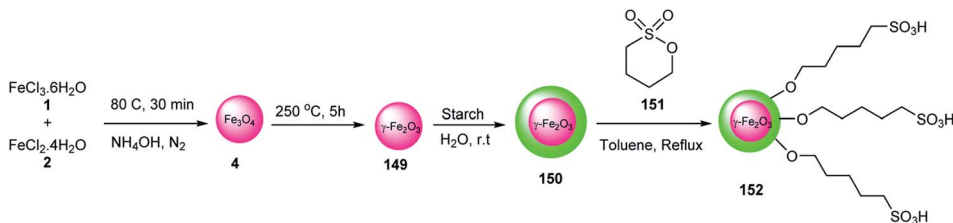
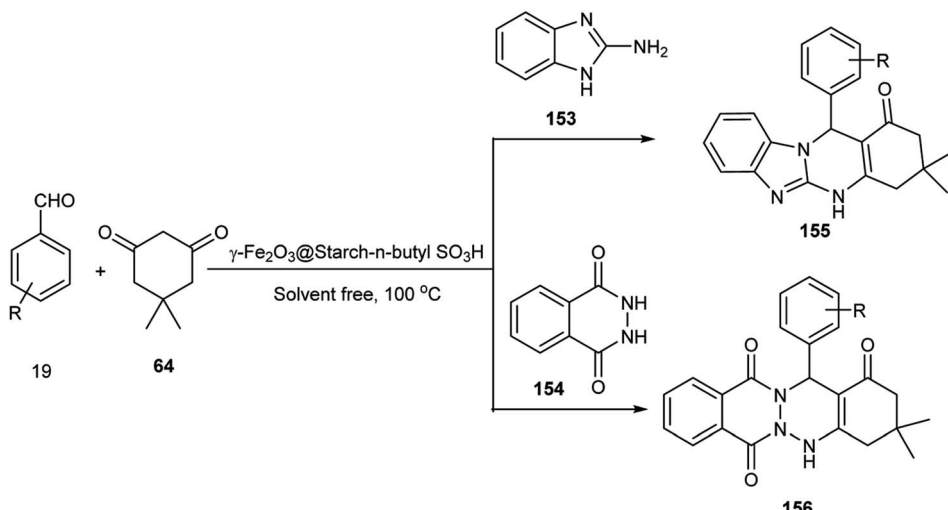
According to the reusability test, this catalyst was used five times without a decrease in any of its activities. The various functional groups including hydroxyl and amine on the

CSSNH@Arg can activate the carbonyl groups *via* hydrogen bonding.⁷⁶

2.6.2. Synthesis and application of Fe₃O₄@C-SO₃H.

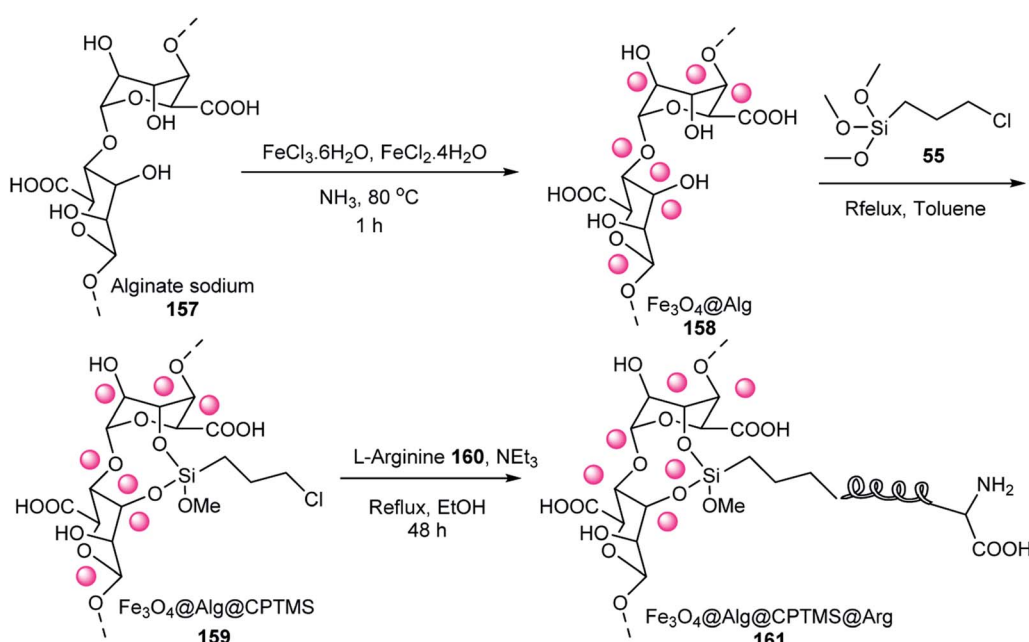
Initially, starch was mixed with sulfuric acid, and then the reaction mixture was transferred to an autoclave for 24 h at 180 °C, resulting in the formation of a solid black product (C-SO₃H). The magnetic Fe₃O₄ nanoparticles, carbon-based solid acid (C-SO₃H) **180**, and H₂O were placed in an oil bath at 100 °C to remove H₂O, and then the reaction mixture was poured into a Teflon-sealed autoclave and heated at 180 °C for 6 h to achieve Fe₃O₄@C-SO₃H **181** (Scheme 57).⁷⁷

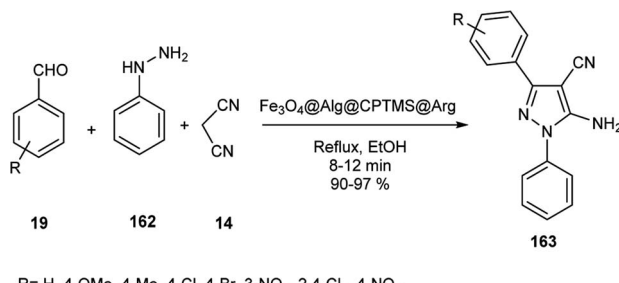
Scheme 44 Synthesis of 2,4,6-triarylpyridine derivatives **148** using Fe₃O₄@GOTfOH/Ag/St-PEG-AcA.

Scheme 45 Synthesis of γ -Fe₂O₃@starch-*n*-butyl SO₃H.Scheme 46 Synthesis of tetrahydrobenzimidazo[2,1-*b*]quinazolin-1(2*H*)-ones 155 or 2*H*-indazolo[2,1-*b*]phthalazine-triones 156 using γ -Fe₂O₃@starch-*n*-butyl SO₃H.

CSSNH was applied as a Brønsted acid catalyst in the synthesis of 2-amino-3-cyano-4*H*-pyrans 126 and 2-amino-4*H*-chromenes 116 or 182 *via* the three-component reactions of malononitrile 14,

benzaldehyde 19, and β -naphthol 101 or dimedone 64 or 4-hydroxycoumarin 124, respectively (Scheme 58). This catalyst was used four times without any loss in its activity.⁷⁷

Scheme 47 Synthesis of Fe₃O₄@Alg@CPTMS@Arg 161.



Scheme 48 Synthesis of 2,4,5-triarylimidazoles 163 using $\text{Fe}_3\text{O}_4@\text{Alg}@\text{CPTMS}@\text{Arg}$.

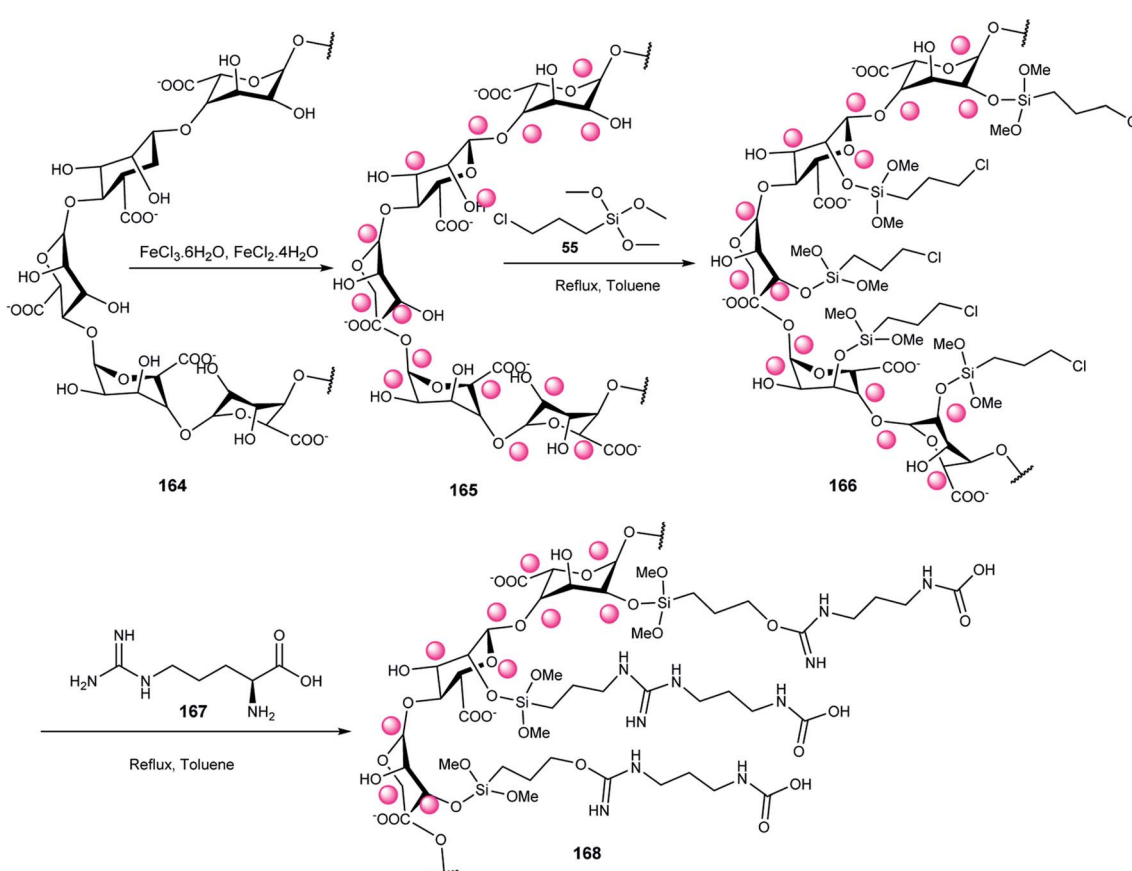
2.6.3. Synthesis and application of magnetic chitosan-terephthaloyl-creatine bio-nanocomposite. The reaction of terephthaloyl chloride 183 and creatine powders 184 in CH_2Cl_2 under reflux conditions provided creatine-terephthaloyl chloride ligand 185, which was added to chitosan 176 powder in a hydrochloric acid solution, and then refluxed to give chitosan-terephthaloyl-creatine bio-nanocomposite 186, followed by immobilization on Fe_3O_4 to provide magnetic chitosan-terephthaloyl-creatine bio-nanocomposite 187 (Scheme 59).⁷⁸

Its catalytic activity was tested in the synthesis of poly-hydroquinolines 72 *via* the reaction of aldehydes 19, dimedone 67, ammonium acetate 71, and ethyl acetoacetate or methyl acetoacetate 21 in EtOH (Scheme 60). In another attempt, it was

used in the synthesis of 1,4-dihydropyridines 73 *via* the pseudo-three-component reaction of aldehydes 19, methyl acetoacetate 21, and ammonium acetate 71 (Scheme 61). The acidic site of the catalyst activated the carbonyl groups of the primary compounds. The activity of this catalyst did not decrease after use eight times.⁷⁸

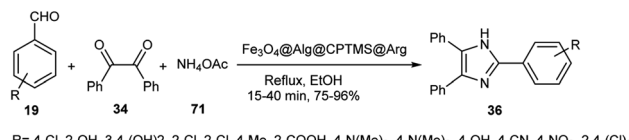
2.6.4. Synthesis and application of magnetic cyanoguanidine-modified chitosan (MCGC). Firstly, chitosan 176 was obtained *via* the deacetylation of chitin 74, and then it was modified by treatment with cyanoguanidine 188 in HCl solution to produce cyanoguanidine-modified chitosan (CGC) 189, which was immobilized on Fe_3O_4 nanoparticles to afford magnetic cyanoguanidine-modified chitosan (MCGC) 190 (Scheme 62). Its catalytic activity was investigated in the synthesis of benzimidazoloquinazolines 155 *via* the reaction of aldehydes 19, 2-aminobenzimidazole 153, and dimedone 64 in EtOH under reflux conditions. The sonochemical method afforded better yields in shorter reaction times than the conventional method (Scheme 63).⁷⁹

1,4-Dihydropyridines 73 were synthesized *via* the Hantzsch reaction of ethyl acetoacetate 35, aromatic aldehydes 19, and ammonium acetate 71 under ultrasonic irradiation in the presence of MCGC 190 as a catalyst, which activated the carbonyl groups *via* hydrogen bonding. Also, the yield of the reaction did not decrease after eight times usage of the catalyst (Scheme 64).⁷⁹



Scheme 49 Synthesis of $\text{Fe}_3\text{O}_4@\text{Alg}@\text{CPTMS}@\text{Arg}$.

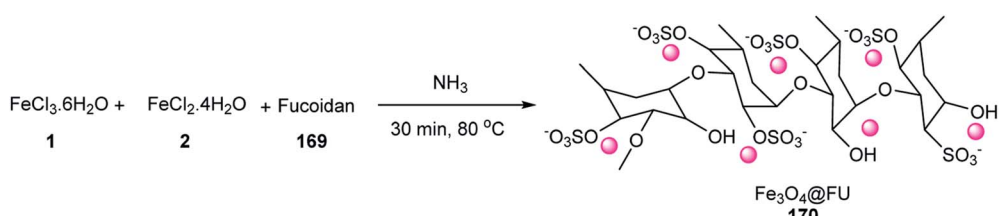




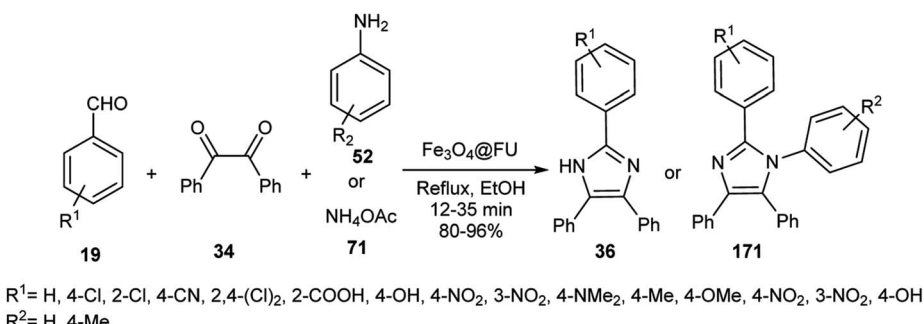
Scheme 50 Synthesis of 2,4,5-triarylimidazoles derivatives in the presence of $\text{Fe}_3\text{O}_4@\text{Alg}@$ CPTMS.

2.6.5. Synthesis and application of magnetic MnFe_2O_4 -CS-Bu-SO₃H. Manganese ferrite nanoparticles were synthesized *via* the co-precipitation of Fe(III) **1** and Mn(II) **189** in the presence of NaOH solution at 97 °C to give MnFe_2O_4 **191**, which was immobilized on chitosan **176** and 4-butane sultone **151** to prepare MnFe_2O_4 -CS-Bu-SO₃H **192** (Scheme 65).⁸⁰

The catalyst activity of MnFe_2O_4 -CS-Bu-SO₃H was investigated in the synthesis of *spiro*[acenaphthylene-1,9'-acridine]



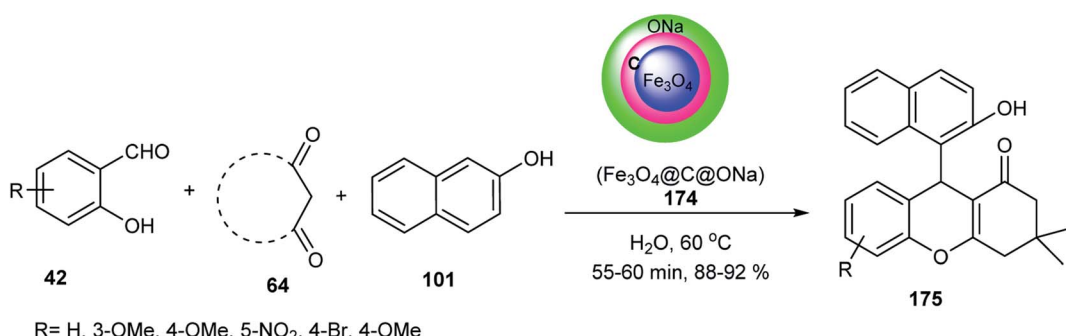
Scheme 51 Synthesis of magnetic $\text{Fe}_3\text{O}_4@\text{FU}$ **170**.



Scheme 52 Synthesis of imidazole derivatives.

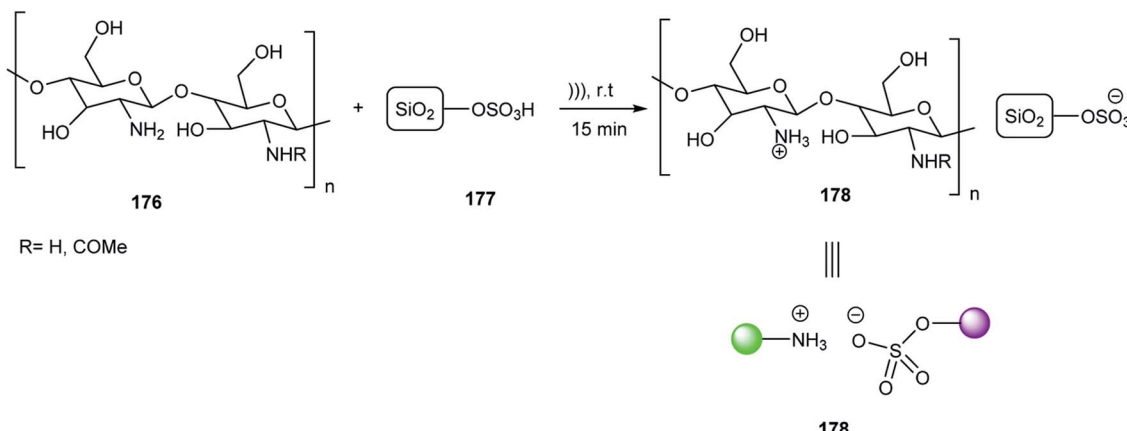


Scheme 53 Synthesis of $\text{Fe}_3\text{O}_4@\text{C@ONa}$.

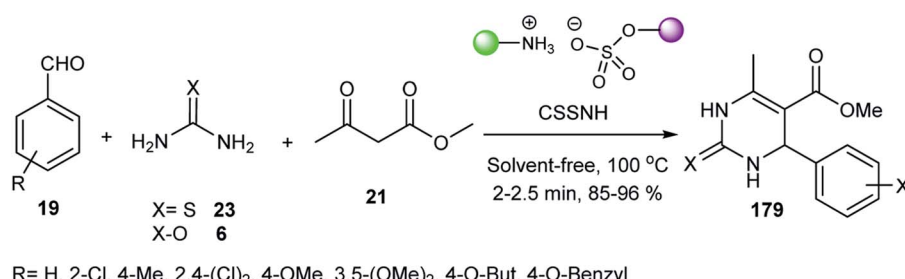


Scheme 54 Synthesis of 4H-chromene derivatives using $\text{Fe}_3\text{O}_4@\text{C@ONa}$ **174**.





Scheme 55 Synthesis of CSSNH@Arg 178.



Scheme 56 Synthesis of 3,4-dihydropyrimidine-2(1H)-(thio)ones using of CSSNH@Arg 178.

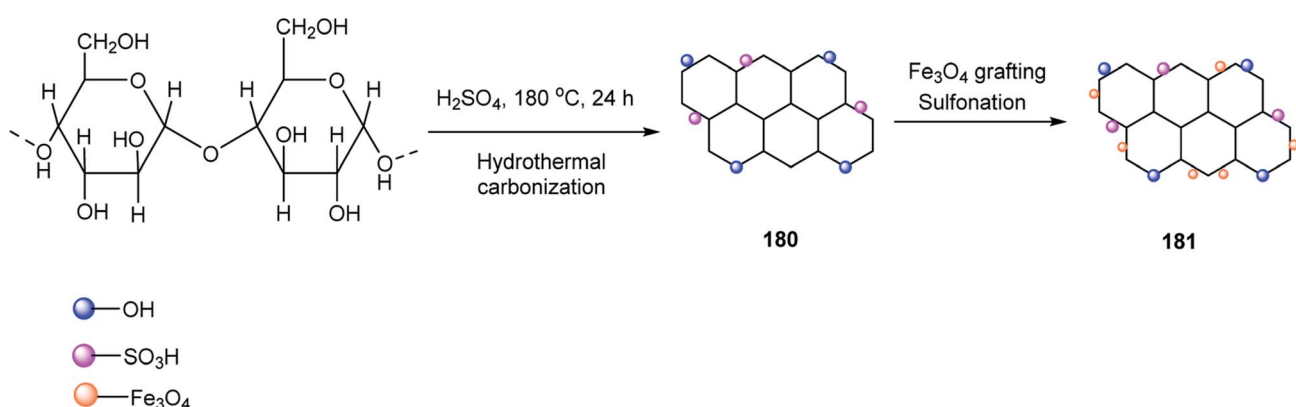
triones **194** *via* the multicomponent reaction of dimedone **64**, aldehydes **19**, and acenaphthoquinone **193** under ultrasonic irradiation in H₂O (Scheme 66). Also, MnFe₂O₄-CS-Bu-SO₃H as a Brønsted acid increased the reaction rate *via* hydrogen bonding with the carbonyl group. According to the reusability test, this catalyst was used five times without any loss in its activity.⁸⁰

2.6.6. Synthesis and application of magnetic Cu-MCS. Fe₃O₄ NPs **4** were reacted with carboxymethylated chitosan to obtain magnetic chitosan MCS **195**, which was reacted with

CuCl₂·2H₂O in H₂O to generate Cu NPs@Fe₃O₄-chitosan (Cu-MCS) **196** (Scheme 67).

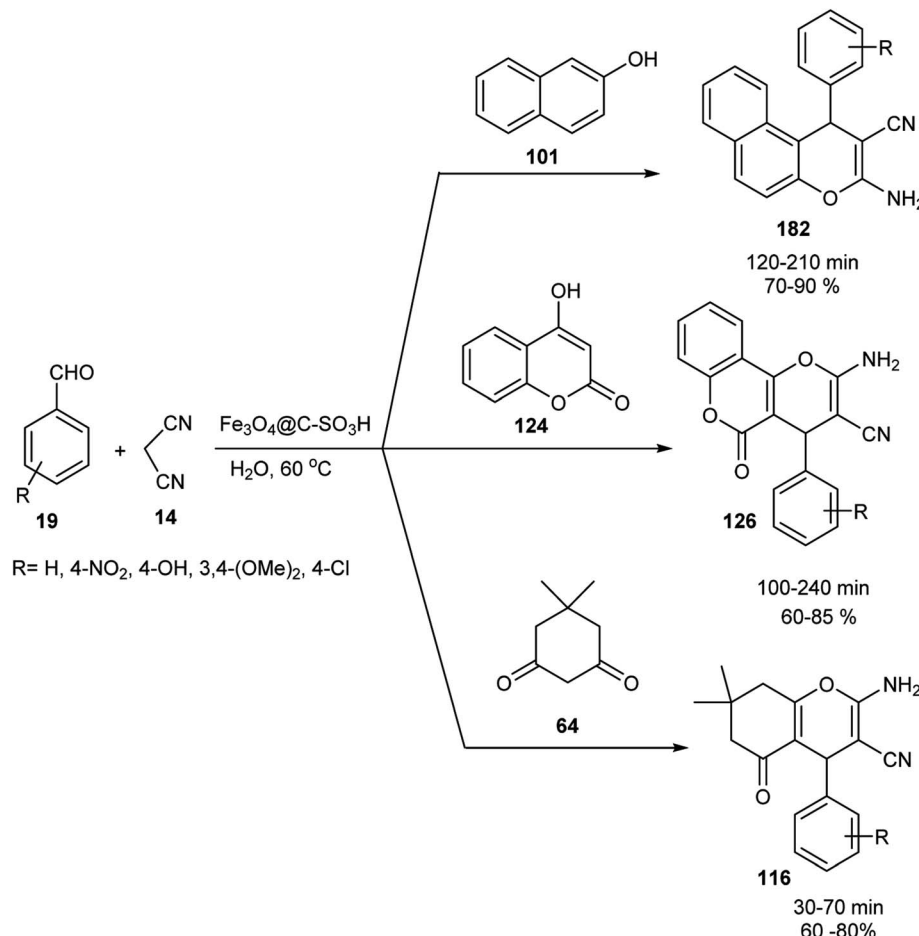
The catalytic activity of Cu-MCS was verified in the synthesis of various tetrazoles **198** or **199** *via* the reaction of cyanamides **197** and NaN₃ **50** in H₂O under reflux conditions (Scheme 68). This catalyst could be used five times without loss in its activity.⁸¹

2.6.7. Synthesis and application of magnetic Ch-Fe₃O₄ NCs. Chitosan was dissolved in an acetic acid solution, and then FeCl₃·6H₂O **1** and FeCl₂·4H₂O **2** were added to the reaction mixture for 6 h at 80 °C under an N₂ atmosphere. Then, NH₄OH

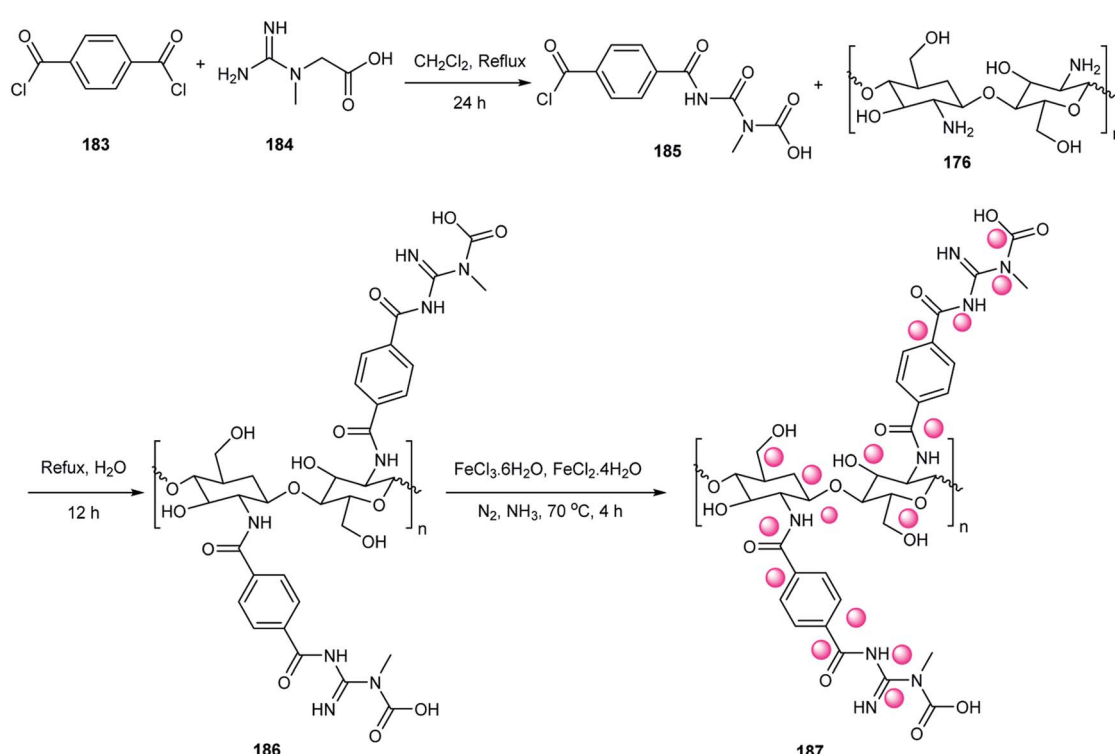


Scheme 57 Synthesis of 3,4-dihydropyrimidine-2(1H)-(thio)ones in the presence of CSSNH 178.



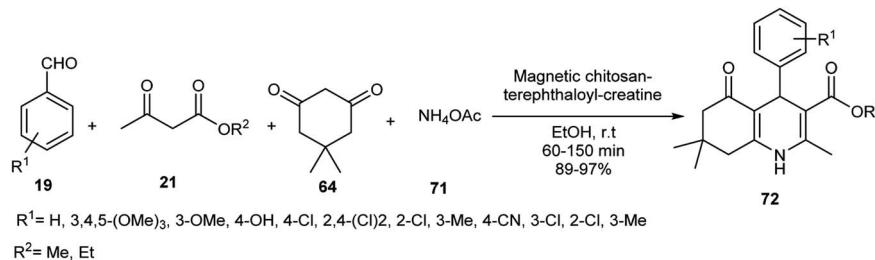


Scheme 58 Synthesis of 2-amino-4H-chromenes **116** and 2-amino-3-cyano-4H-pyrans **126** in the presence of $\text{Fe}_3\text{O}_4@\text{C-SO}_3\text{H}$.

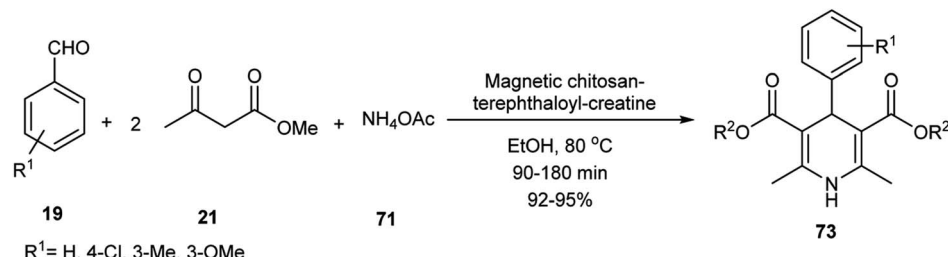


Scheme 59 Synthesis of magnetic chitosan-terephthaloyl-creatine bio-nanocomposite.





Scheme 60 Synthesis of polyhydroquinoline derivatives 72.



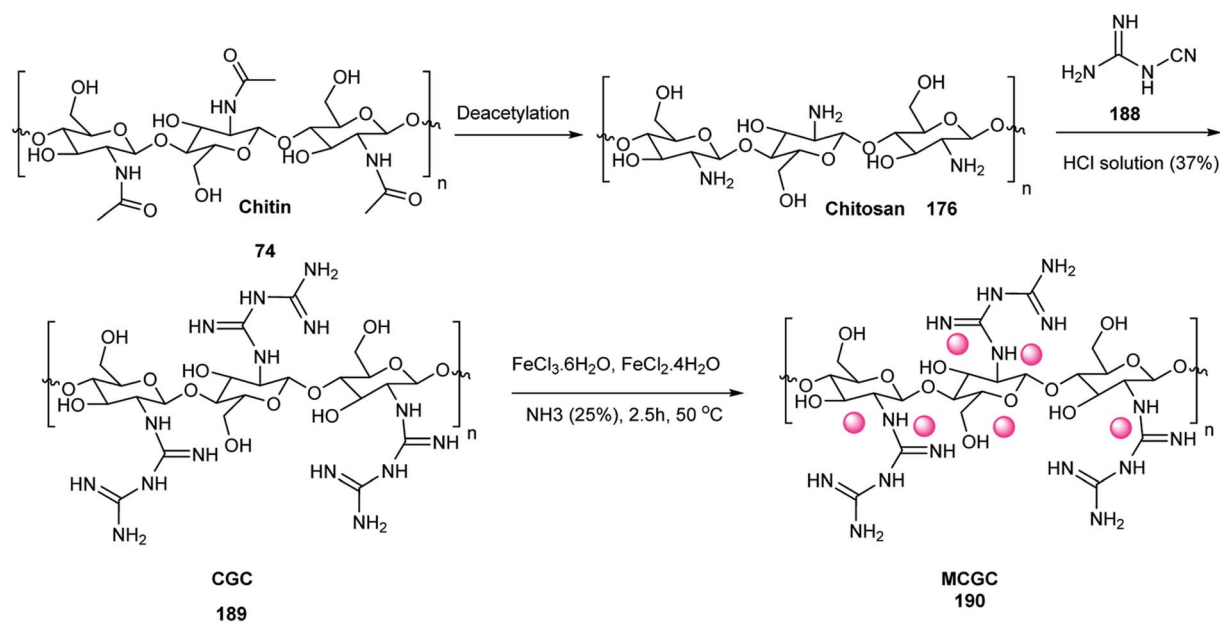
Scheme 61 Synthesis of 1,4-dihydropyridine derivatives 73 in the presence of terephthaloyl-creatine bio-nanocomposite.

was added to the reaction mixture to obtain $\text{Ch}-\text{Fe}_3\text{O}_4$ NCs **200**. Finally, the chitosan magnetic nanocomposite of Ch -rhomboclase NCs **201** was synthesized *via* the reaction of $\text{Ch}-\text{Fe}_3\text{O}_4$ NCs **200** with chlorosulfonic acid at room temperature under N_2 gas (Scheme 69).⁸²

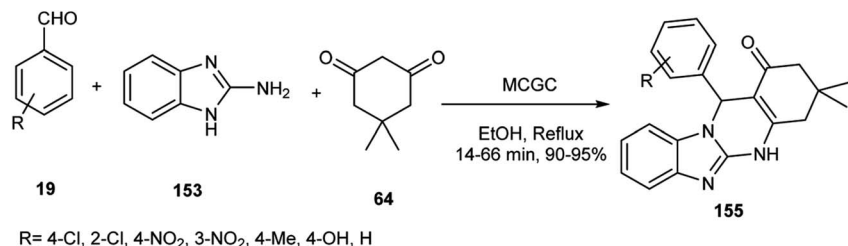
The condensation reaction of benzaldehyde **19**, ethyl acetacetate **35** or dimedone **64**, and ammonium acetate **71** gave 1,4-dihydropyridine derivatives **73** or **202** in the presence of Ch -

rhomboclase NCs **201** under solvent-free conditions at $80\text{ }^\circ\text{C}$ (Scheme 70). In the Hantzsch reaction, this acidic catalyst activated carbonyl groups *via* hydrogen bonding. Also, according to the reusability test, the catalyst was used seven times without any decrease in its activity.⁸²

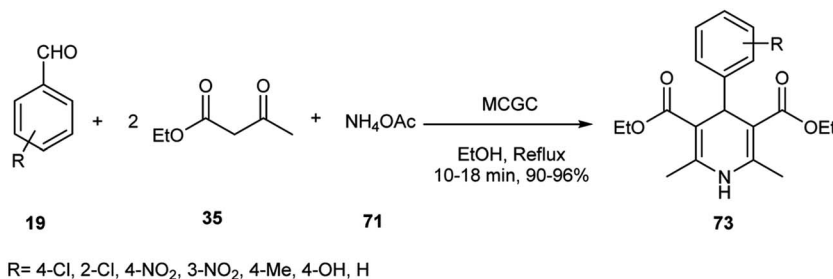
2.6.8. Synthesis and application of magnetic $\text{Fe}_3\text{O}_4/\text{CS}/\text{COF/Cu}$. After the preparation of an $\text{FeCl}_3 \cdot 6\text{H}_2\text{O}$ solution in ethylene glycol at room temperature, chitosan, sodium acetate,



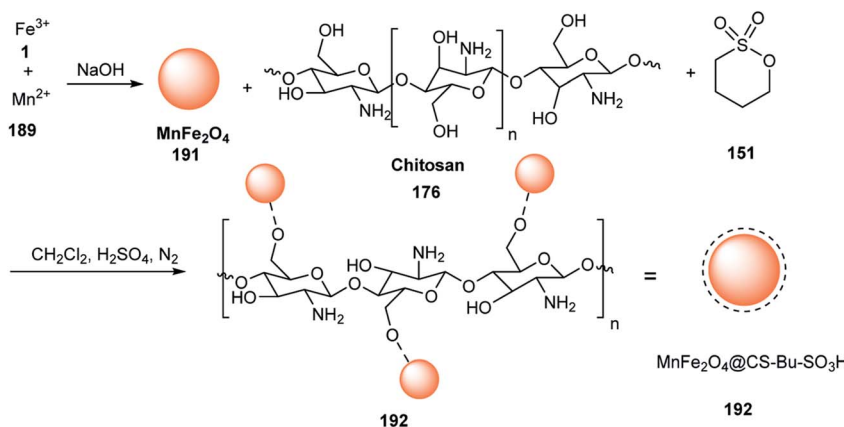
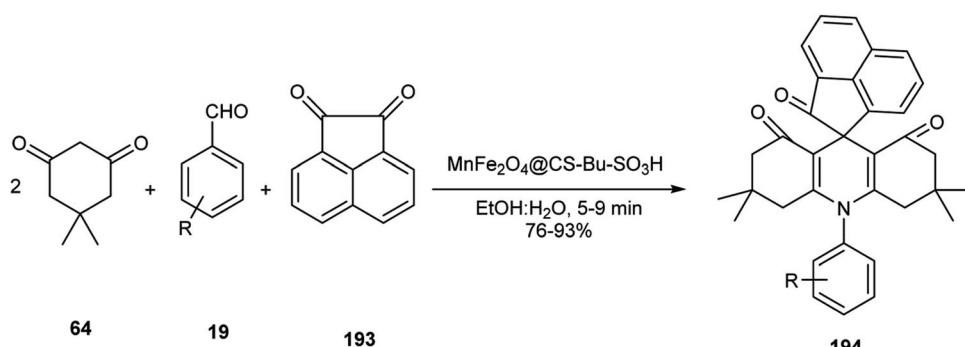
Scheme 62 Synthesis of magnetic cyanoguanidine-modified chitosan (MCGC).

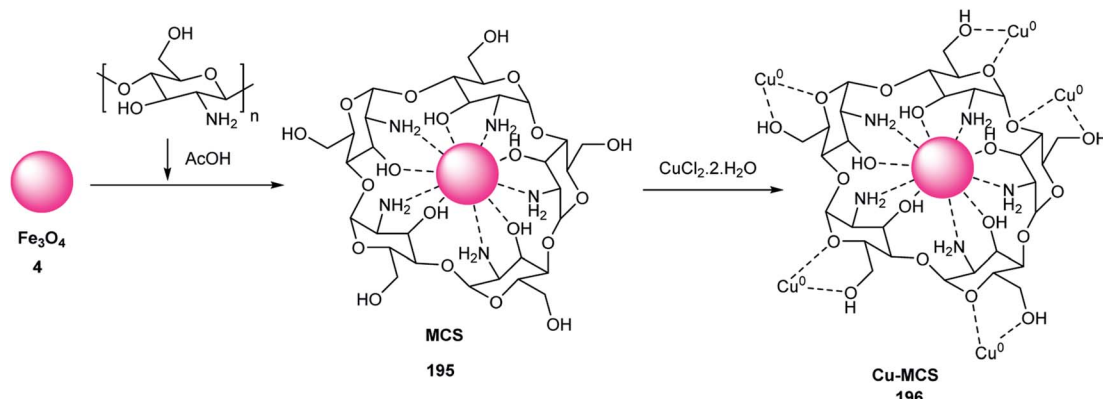


Scheme 63 Synthesis of benzimidazoloquinazoline derivatives.

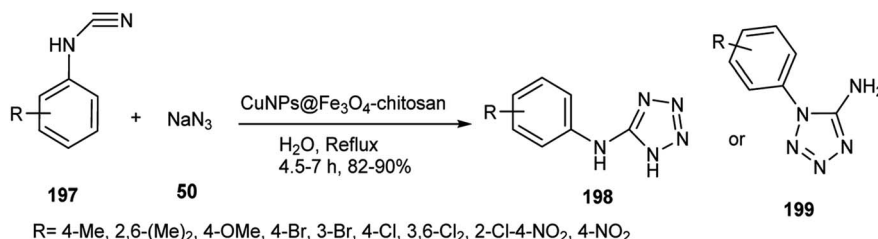


Scheme 64 Synthesis of 1,4-dihydropyridines.

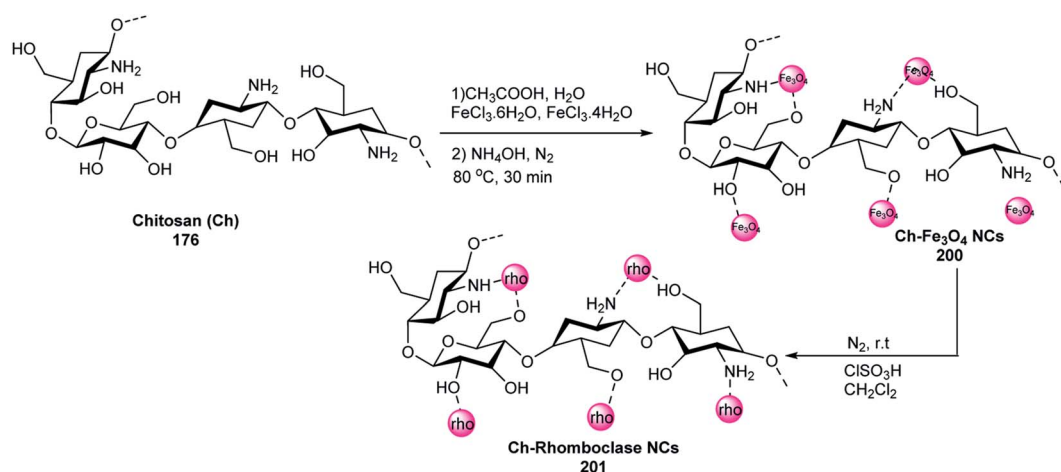
Scheme 65 Synthesis of MnFe₂O₄-CS-Bu-SO₃H 192.Scheme 66 Synthesis of spiro[acenaphthylene-1,9'-acridine] triones 194 in the presence of MnFe₂O₄@CS-Bu-SO₃H NPs.



Scheme 67 Synthesis of Cu-MCS.



Scheme 68 Synthesis of various tetrazoles 198 or 199 using Cu-MCS.

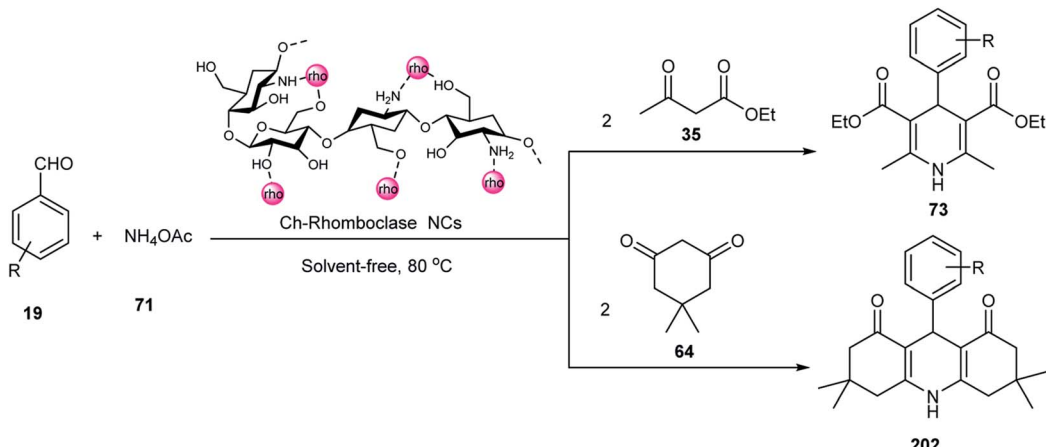


Scheme 69 Synthesis of Ch-rhomboclase NCs 201.

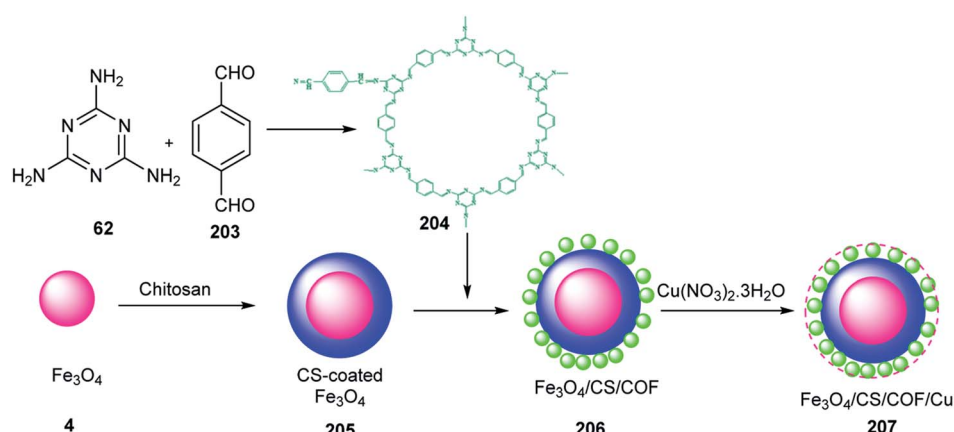
and ethylenediamine were added to it. Then, this mixture was placed in a Teflon-lined autoclave and heated at 200 °C for 8 h to obtain $\text{Fe}_3\text{O}_4/\text{CS}$ 205, which was dispersed in DMSO under ultrasound irradiation to give CS-coated Fe_3O_4 , followed by mixing with melamine 63 and terephthalaldehyde 203. The obtained mixture was transferred in a Teflon-lined autoclave at 180 °C for 12 h to obtain $\text{Fe}_3\text{O}_4/\text{CS}/\text{COF}$ 206, which was reacted with $\text{Cu}(\text{NO}_3)_2 \cdot 3\text{H}_2\text{O}$ in EtOH under reflux conditions and

argon atmosphere for 24 h to generate $\text{Fe}_3\text{O}_4/\text{CS}/\text{COF}/\text{Cu}$ 207 (Scheme 71).⁸³

The catalytic activity of $\text{Fe}_3\text{O}_4/\text{CS}/\text{COF}/\text{Cu}$ 207 was tested in the synthesis of polyhydroquinolines 72 *via* the Hantzsch reaction of aldehydes 19, dimedone 64, ammonium acetate 71, and ethyl acetoacetate 35 (Scheme 72). $\text{Fe}_3\text{O}_4/\text{CS}/\text{COF}/\text{Cu}$ with two sites including a Lewis acid (Cu^{2+}) and Lewis base (imine) catalyzed the Hantzsch reaction, which was used five times without a decrease in its activity.⁸³



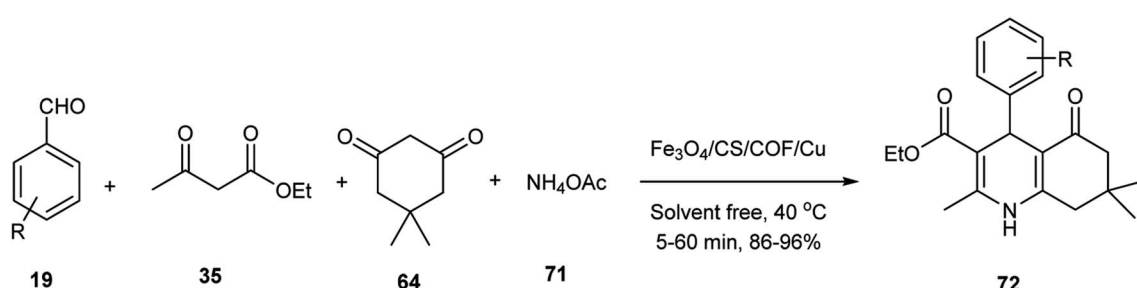
Scheme 70 Synthesis of 1,4-dihydropyridine derivatives 73 or 202.

Scheme 71 Synthesis of the $\text{Fe}_3\text{O}_4/\text{CS}/\text{COF}/\text{Cu}$.

2.7. Synthesis and application of magnetic $\text{ZnS}/\text{CuFe}_2\text{O}_4/\text{agar}$

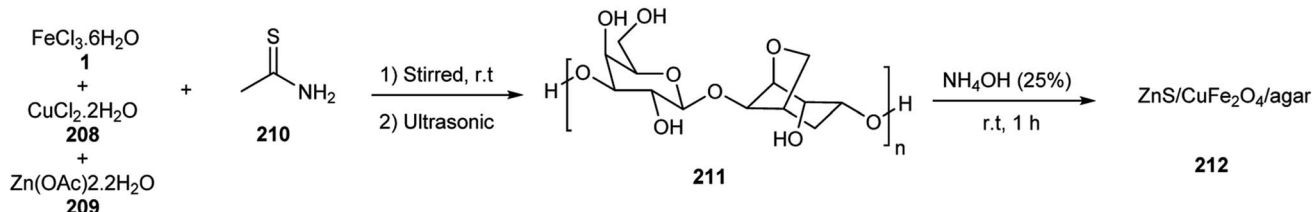
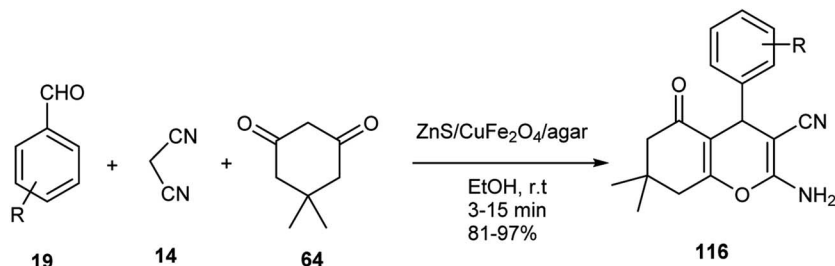
$\text{FeCl}_3 \cdot 6\text{H}_2\text{O}$ 1, $\text{CuCl}_2 \cdot 2\text{H}_2\text{O}$ 208, $\text{Zn}(\text{OAc})_2 \cdot 2\text{H}_2\text{O}$ 209, and thiourea were dissolved in distilled H_2O . Then, agar 211 and ammonia solution were added to the reaction mixture to obtain $\text{ZnS}/\text{CuFe}_2\text{O}_4/\text{agar}$ 212 (Scheme 73).⁸⁴

The catalytic activity of $\text{ZnS}/\text{CuFe}_2\text{O}_4/\text{agar}$ 212 was examined in the reaction of dimedone 64, malononitrile 14, and aldehydes 19 to synthesize 2-amino-tetrahydro-4*H*-chromene-3-carbonitriles 116 (Scheme 74). The carbonyl groups were activated in the presence of $\text{ZnS}/\text{CuFe}_2\text{O}_4$ via interaction with the hydroxyl groups of agar and Zn metal as a Lewis acid. The catalyst was reused five times with no reduction in its activity.⁸⁴



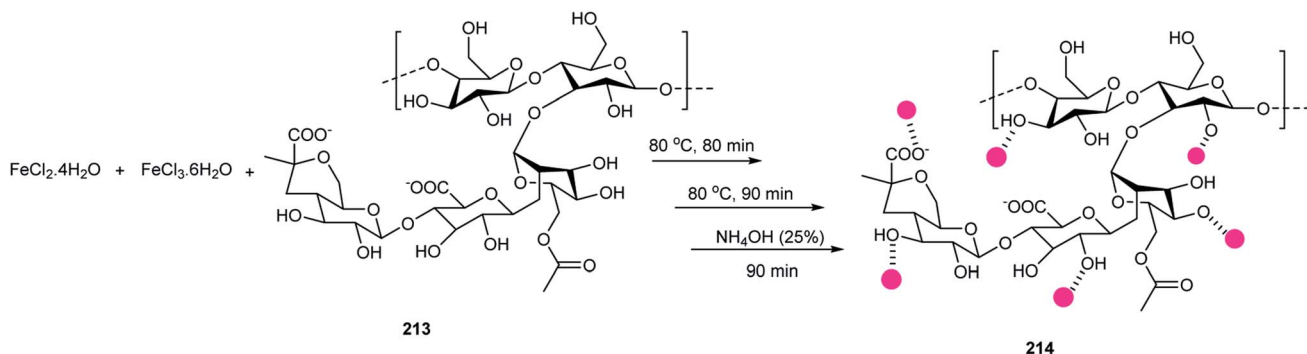
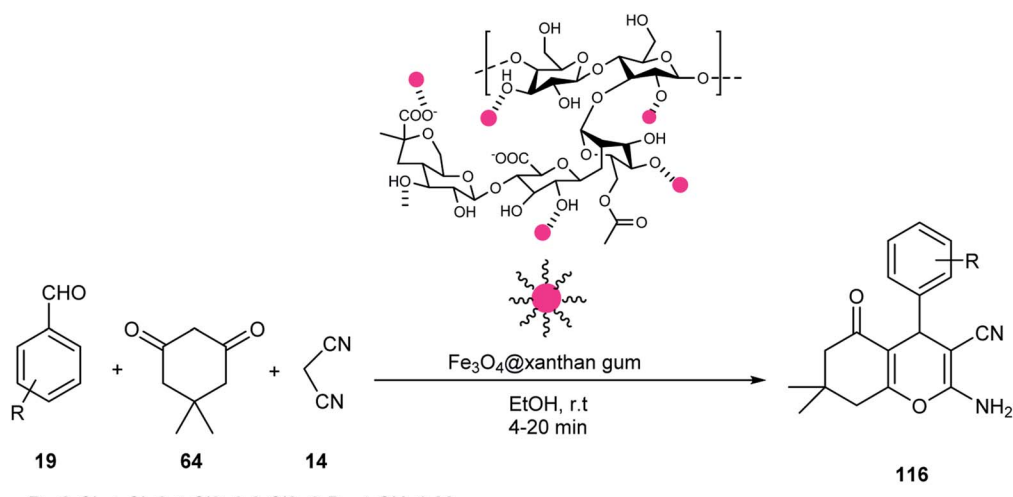
R= H, 4-NO₂, 2-C, 4-Cl, 3-Br, 4-Me, 4-OMe, 2-OMe, 2-OH

Scheme 72 Synthesis of polyhydroquinoline derivatives via Hantzsch reaction.

Scheme 73 Synthesis of ZnS/CuFe₂O₄/agar 212.

R= 4-NO₂, 3-NO₂, 2-Cl, 3-Cl, 4-Cl, 3-Me, 4-Me, 4-CH(Me)₂, 2-OMe, 3-OMe, 4-OMe, 3,4,5-(OMe)₃, 3-OH, 4-OH, 2,4-Cl₂

Scheme 74 Synthesis of 2-amino-tetrahydro-4H-chromene-3-carbonitrile derivatives.

Scheme 75 Synthesis of Fe₃O₄@xanthan gum 214.

R= 2-Cl, 4-Cl, 2,4-Cl₂, 2,6-Cl₂, 2-Br, 4-CN, 3-Me

Scheme 76 Synthesis of 2-amino-3-cyano-4H-pyran derivatives 116 using Fe₃O₄@xanthan gum.

2.8. Synthesis and application of magnetic $\text{Fe}_3\text{O}_4@\text{xanthan}$ gum

NH_4OH solution was added to a mixture of the $\text{FeCl}_2 \cdot 4\text{H}_2\text{O}$, $\text{FeCl}_3 \cdot 6\text{H}_2\text{O}$ (1 : 2), and an aqueous suspension of xanthan gum 213 to give $\text{Fe}_3\text{O}_4@\text{xanthan}$ gum 214 (Scheme 75).⁸⁵

$\text{Fe}_3\text{O}_4@\text{xanthan}$ gum was applied in the synthesis of 2-amino-3-cyano-4H-pyran derivatives 116 via the reaction of aldehydes 19, dimedone 64, and malononitrile 14 in EtOH (Scheme 76). The model reaction was performed about nine times and the yields did not decrease. This reaction was accomplished in the presence of Fe_3O_4 after 45 min in 30% yield. It was shown that $\text{Fe}_3\text{O}_4@\text{xanthan}$ gum activated the carbonyl groups via hydrogen bonding, which was more effective than Fe_3O_4 .⁸⁵

3. Conclusion

Many bio-polymers can be obtained from natural sources. According to the importance of green chemistry in organic reactions, in this review, the application of bio-polymers as a catalyst in multicomponent reactions was grouped and summarized. Herein, we highlighted the immobilization of magnetic nanoparticles with bio-polymers. Due to the excellent properties of magnetic nano-catalysts, including their non-toxic nature, high surface area, simple preparation, easy surface modification, and simple separation, these systems have been applied as catalysts in multicomponent reactions. Various organic compounds such as bio-polymers were used for the modification of magnetic nanoparticles. Bio-polymers have various advantages such as biodegradable, biocompatible, and heat-resistant nature. Therefore, herein, their synthesis and catalytic activities in multicomponent reactions were studied. We believe that this article will guide researchers in the design and synthesis of various compounds according to green chemistry. Magnetic nanocomposites have many applications in various fields including, drug delivery, solar cells, chemical sensors, water treatment, biomedical sensors, and catalysts. The importance of these topics could be discussed as a review article in the future.

Conflicts of interest

There are no conflicts to declare.

Acknowledgements

We are grateful for the Research Council's support of Alzahra University.

References

- 1 A. Ali, H. Zafar, M. Zia, U. HAQ, A. Phull, J. Ali and A. Hussain, *Nanotechnol. Sci. Appl.*, 2016, **9**, 49–67.
- 2 F. Erogogbo, K.-T. Yong, R. Hu, W.-C. Law, H. Ding, C.-W. Chang, P. N. Prasad and M. T. Swihart, *ACS Nano*, 2010, **4**, 5131–5138.
- 3 M. Esmaeilpour, J. Javidi, F. N. Dodeji and H. Hassannezhad, *J. Iran. Chem. Soc.*, 2014, **11**, 1703–1715.
- 4 L. Lai, Q. Xie, L. Chi, W. Gu and D. Wu, *J. Colloid Interface Sci.*, 2016, **465**, 76–82.
- 5 A. Abou-Hassan, O. Sandre, S. Neveu and V. Cabuil, *Angew. Chem.*, 2009, **121**, 2378–2381.
- 6 N. O. Mahmoodi, F. Ghanbari Pirbasti and Z. Jalalifard, *J. Chin. Chem. Soc.*, 2018, **65**, 383–394.
- 7 M. Esmaeilpour, J. Javidi and M. Zandi, *New J. Chem.*, 2015, **39**, 3388–3398.
- 8 X. Chen, Y. Zhou, H. Han, X. Wang, L. Zhou, Z. Yi and L. Zeng, *Mater. Today Chem.*, 2021, **22**, 100556.
- 9 G. U. I. Sheng, S. H. E. N. Xiaodong and L. I. N. Benlan, *Rare Met.*, 2006, **25**, 426–430.
- 10 S. S. Khasraghi, M. Shojaei, M. Janmaleki and U. Sundararaj, *Eur. Polym. J.*, 2021, **159**, 110735.
- 11 X. Liu, J. Tian, Y. Li, N. Sun, S. Mi, Y. Xie and Z. Chen, *J. Hazard. Mater.*, 2019, **373**, 397–407.
- 12 M. Muthiah, I. K. Park and C. S. Cho, *Biotechnol. Adv.*, 2013, **3**, 1224–1236.
- 13 R. Mohammadi, A. Saboury, S. Javanbakht, R. Foroutan and A. Shaabani, *Eur. Polym. J.*, 2021, **153**, 110500.
- 14 M. A. Almessiere, Y. Slimani, A. Demir Korkmaz, A. Baykal, H. Albetran, T. A. Saleh, M. Sertkol and I. Ercan, *Ultrason. Sonochem.*, 2020, **62**, 104847.
- 15 H. Javadian, M. Ruiz, T. A. Saleh and A. M. Sastre, *J. Mol. Liq.*, 2020, **306**, 112760.
- 16 A. A. Basaleh, M. H. Al-Malack and T. A. Saleh, *J. Environ. Chem. Eng.*, 2021, **9**, 105126.
- 17 A. A. Basaleh, M. H. Al-Malack and T. A. Saleh, *Sustainable Chem. Pharm.*, 2021, **23**, 100503.
- 18 N. Dhenadhyalan, K. C. Lin and T. A. Saleh, *Small*, 2020, **6**, 1905767.
- 19 A. M. Alansi, M. Al-Qunaibit, I. O. Alade, T. F. Qahtan and T. A. Saleh, *J. Mol. Liq.*, 2018, **253**, 297–304.
- 20 A. M. Alansi, T. F. Qahtan and T. A. Saleh, *Adv. Mater. Interfaces*, 2021, **8**, 2001463.
- 21 A. M. Alansi, T. F. Qahtan, N. Al Abass, J. M. AlGhamdi, M. Al-Qunaibit and T. A. Saleh, *Adv. Sustainable Syst.*, 2021, **2100267**.
- 22 T. A. Saleh, *Environ. Technol. Innovation*, 2021, **24**, 101821.
- 23 J. Wang, Z. Shi, J. Fan, Y. Ge, J. Yin and G. Hu, *J. Mater. Chem.*, 2012, **22**, 22459.
- 24 T. A. Debele, S. L. Mekuria and H. C. Tsai, *Mater. Sci. Eng., C*, 2016, **68**, 964–981.
- 25 A. Maleki and M. Kamalzare, *Catal. Commun.*, 2014, **53**, 67–71.
- 26 V. Omid, F. M. Kievit, C. Fang, N. Mu, S. Jana, M. C. Leung, H. Mok, R. G. Ellenbogen, J. O. Park and M. Zhang, *Biomaterials*, 2010, **31**, 8032–8042.
- 27 Z. M. Avval, L. Malekpour, F. Raeisi, A. Babapoor, S. M. Mousavi, S. A. Hashemi and M. Salari, *Drug Metab. Rev.*, 2020, **52**, 157–184.
- 28 S. Mirza, M. S. Ahmad, M. I. A. Shah and M. Ateeq, In *Metal nanoparticles for drug delivery and diagnostic applications*, Elsevier, 2020, pp. 189–213.



29 A. Gholami, S. M. Mousavi, S. A. Hashemi, Y. Ghasemi, W.-H. Chiang and N. Parvin, *Drug Metab. Rev.*, 2020, **52**, 205–224.

30 X. Sun, G. Zhang, R. Du, R. Xu, D. Zhu, J. Qian, G. Bai, C. Yang, Z. Zhang, X. Zhang and D. Zou, *Biomaterials*, 2019, **194**, 151–160.

31 Z. Zhou, L. Yang, J. Gao and X. Chen, *Adv. Mater.*, 2019, **31**, 1804567.

32 D. D. Stueber, J. Villanova, I. Aponte, Z. Xiao and V. L. Colvin, *Pharmaceutics*, 2021, **13**, 943.

33 N. M. El-Shafai, M. M. Abdelfatah, M. E. El-Khouly, I. M. El-Mehasseb, A. El-Shaer, M. S. Ramadan, M. S. Masoud and M. A. El-Kemary, *Appl. Surf. Sci.*, 2020, **506**, 144896.

34 L. Gloag, M. Mehdipour, D. Chen, R. D. Tilley and J. J. Gooding, *Adv. Mater.*, 2019, **31**, 1904385.

35 S. Khizar, H. Ben Halima, N. M. Ahmad, N. Zine, A. Errachid and A. Elaissari, *Electrophoresis*, 2020, **41**, 1206–1224.

36 M. P. Conte, J. K. Sahoo, Y. M. Abul-Haija, K. A. Lau and R. V. Ulijn, *ACS Appl. Mater. Interfaces*, 2018, **10**, 3069–3075.

37 S. Mallakpour and M. Hatami, *Appl. Clay Sci.*, 2019, **174**, 127–137.

38 N. Shabani, A. Javadi, H. Jafarizadeh-Malmiri, H. Mirzaei and J. Sadeghi, *Food Hyg.*, 2021, **10**, 61–71.

39 R. Banerjee, Y. Katsenovich, L. Lagos, M. McIntosh, X. Zhang and C.-Z. Li, *Curr. Med. Chem.*, 2010, **17**, 3120–3141.

40 S. Mallakpour, M. Tukhani and C. M. Hussain, *Int. J. Biol. Macromol.*, 2021, **179**, 429.

41 S. Kamel and T. A. Khattab, *Cellulose*, 2021, **28**, 4545.

42 G. Mohammadi Ziarani, Z. Kheirkordi, F. Mohajer, A. Badiei and R. Luque, *RSC Adv.*, 2021, **11**, 17456–17477.

43 G. Mohammadi Ziarani, S. Rohani, A. Ziarati and A. Badiei, *RSC Adv.*, 2018, **8**, 41048–41100.

44 F. Mohajer, G. Mohammadi Ziarani and A. Badiei, *RSC Adv.*, 2021, **11**, 6517–6525.

45 Z. Kheirkordi, G. Mohammadi Ziarani and F. Mohajer, *Curr. Org. Chem.*, 2022, **26**, 287–298.

46 G. Mohammadi Ziarani, R. Moradi, T. Ahmadi and N. Lashgari, *RSC Adv.*, 2018, **8**, 12069–12103.

47 G. Mohammadi Ziarani, F. Aleali and N. Lashgari, *RSC Adv.*, 2016, **6**, 50895–50922.

48 G. Mohammadi Ziarani, N. H. Nasab and N. Lashgari, *RSC Adv.*, 2016, **6**, 38827–38848.

49 L. A. Thompson, *Curr. Opin. Chem. Biol.*, 2000, **4**, 324–337.

50 A. Dömling, *Curr. Opin. Chem. Biol.*, 2002, **6**, 306–313.

51 E. Zare and Z. Rafiee, *Appl. Organomet. Chem.*, 2020, **34**, e5516.

52 S. S. Hosseinkhah and B. B. F. Mirjalili, *RSC Adv.*, 2020, **10**, 40508–40513.

53 P. G. Kargar, G. Bagherzade and H. Eshghi, *RSC Adv.*, 2020, **10**, 37086–37097.

54 A. Maleki, S. Gharibi, K. Valadi and R. Taheri-Ledari, *J. Phys. Chem. Solids*, 2020, **142**, 109443.

55 G. Bagherzade, *RSC Adv.*, 2021, **11**, 19203–19220.

56 G. Bagherzade and H. Eshghi, *RSC Adv.*, 2021, **11**, 4339–4355.

57 P. G. Kargar, M. Noorian, E. Chamani, G. Bagherzade and Z. Kiani, *RSC Adv.*, 2021, **11**, 17413–17430.

58 M. Zahedifar, B. Pouramiri and R. Razavi, *Res. Chem. Intermed.*, 2020, **46**, 2749–2765.

59 B. B. F. Mirjalili, Z. Zaghanghi and A. Monfared, *J. Chin. Chem. Soc.*, 2020, **67**, 197–201.

60 N. Safajoo, B. B. F. Mirjalili and A. Bamoniri, *Polycyclic Aromat. Compd.*, 2021, **41**, 1241–1248.

61 N. Safajoo, B. B. F. Mirjalili and A. Bamoniri, *RSC Adv.*, 2019, **9**, 1278–1283.

62 G. Bagherzade and H. Eshghi, *RSC Adv.*, 2020, **10**, 32927–32937.

63 A. D. Tafti and B. B. F. Mirjalili, *RSC Adv.*, 2020, **10**, 31874–31880.

64 A. Maleki, F. Hassanzadeh-Afruzi, Z. Varzi and M. S. Esmaeili, *Mater. Sci. Eng. C*, 2020, **109**, 110502.

65 Z. Amiri-Khamakani, F. Hassanzadeh-Afruzi and A. Maleki, *Chem. Process.*, 2020, **3**, 101.

66 E. Babaei and B. B. F. Mirjalili, *Iran. J. Catal.*, 2020, **10**, 219–226.

67 A. Mohammadzadeh, A. P. Marjani and A. Zamani, *S. Afr. J. Chem.*, 2020, **73**, 55–63.

68 M. Kamalzare, M. Bayat and A. Maleki, *R. Soc. Open Sci.*, 2020, **7**, 200385.

69 M. H. Sayahi, F. Shamkhani, M. Mahdavi and S. Bahadorikhahli, *Starch-Stärke*, 2021, **73**, 2000257.

70 S. Forouzandehdel, M. Meskini and M. R. Rami, *J. Mol. Struct.*, 2020, **1214**, 128142.

71 M. Shamsi-Sani, F. Shirini and M. Mohammadi-Zeydi, *J. Nanosci. Nanotechnol.*, 2019, **19**, 4503–4511.

72 S. Amirnejat, A. Nosrati and S. Javanshir, *Appl. Organomet. Chem.*, 2020, **34**, e5888.

73 S. Amirnejat, A. Nosrati, S. Javanshir and M. R. Naimi-Jamal, *Int. J. Biol. Macromol.*, 2020, **152**, 834–845.

74 M. Banazadeh, S. Amirnejat and S. Javanshir, *Front. Chem.*, 2020, **8**, 1023.

75 H. Ghavidel, B. Mirza and S. Soleimani-Amiri, *Polycycl. Aromat. Compd.*, 2021, **41**, 604–625.

76 S. Behrouz, M. N. Abi and M. A. Piltan, *Acta Chim. Slov.*, 2021, **68**, 374–386.

77 S. Behrouz, M. N. Abi and M. A. Piltan, *J. Appl. Chem.*, 2019, **14**, 109–124.

78 S. Asgharnasl, R. Eivazzadeh-Keihan, F. Radinekiyan and A. Maleki, *Int. J. Biol. Macromol.*, 2020, **144**, 29–46.

79 K. Javanmiri and R. Karimian, *Monatsh. Chem.*, 2020, **151**, 199–212.

80 H. Naeimi and S. Lahouti, *J. Org. Chem. Res.*, 2020, **6**, 54–68.

81 N. Motaharifar, M. Nasrollahzadeh, A. Taheri-Kafrani, R. S. Varma and M. Shokouhimehr, *Carbohydr. Polym.*, 2020, **232**, 115819.

82 P. Kamalzare, B. Mirza and S. Soleimani-Amiri, *J. Nanostructure Chem.*, 2021, **11**, 229–243.

83 E. Zare and Z. Rafiee, *J. Taiwan Inst. Chem. Eng.*, 2020, **116**, 205–214.

84 S. Bahrami, F. Hassanzadeh-Afruzi and A. Maleki, *Appl. Organomet. Chem.*, 2020, **34**, e5949.

85 M. S. Esmaeili, M. R. Khodabakhshi, A. Maleki and Z. Varzi, *Polycyclic Aromat. Compd.*, 2021, **41**, 1953–1971.

